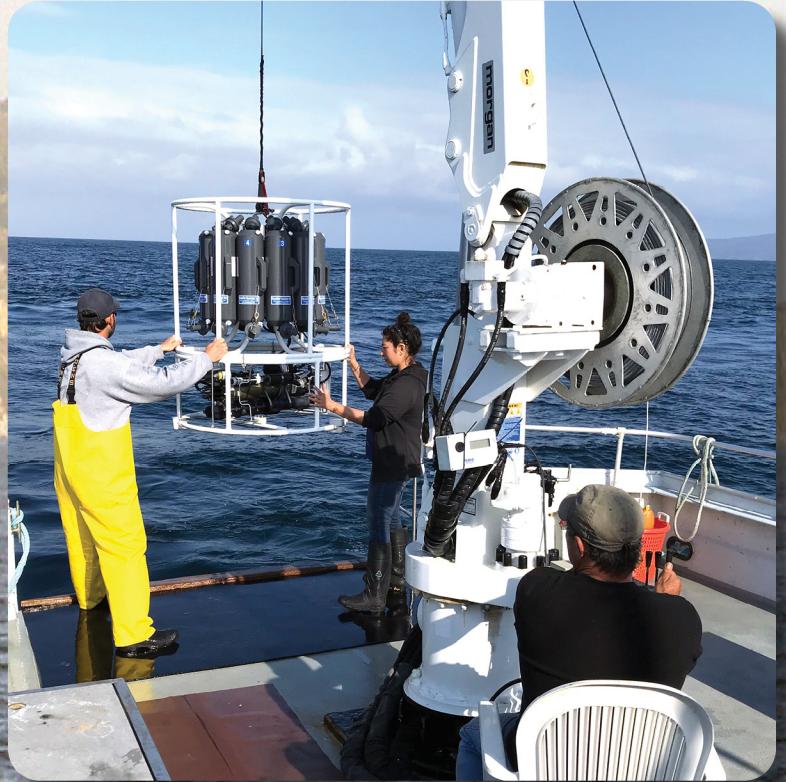# CHAPTER 2
## *Coastal Water Quality*

**Cover Photos**

Upper:      Brent Haggin (Biologist II) and Jovaria Loan (Biologist II), guide the CTD and carousel sampler over the stern while Percival Harper (Boat Deck Hand) operates the crane.

Lower:      Terra Petry (Supervising Biologist) monitors the real time trace of the CTD as it descends through the water column.

# *Chapter 2  Coastal Water Quality*

## INTRODUCTION

The Los Angeles County Sanitation Districts (Sanitation Districts) own and operate the Joint Water Pollution Control Plant (JWPCP), which discharges secondary treated effluent into the Pacific Ocean pursuant to the Waste Discharge Requirements and National Pollutant Discharge Elimination System (NPDES) permit issued by the Los Angeles Regional Water Quality Control Board (LARWQCB; Order No. R4-2017-0180, NPDES No. CA0053813; **Appendix 1.1**). Monitoring and reporting requirements for the NPDES permit are specified in the Monitoring and Reporting Program (MRP) portion of the NPDES permit. The MRP specifies several monitoring elements for the JWPCP, including receiving water (i.e. ocean) monitoring.

The Nearshore/Offshore water quality monitoring program is intended to provide data to determine whether the California Ocean Plan (COP) limits for dissolved oxygen (DO) and pH are being met, and whether sufficient light is present to assure protection of healthy algal communities. The COP limits are set to ensure the reasonable protection of beneficial uses listed in the Water Quality Control Plan for the Los Angeles Region, including boating and water contact recreation, fishing, shellfish harvesting and protection of wildlife and habitat.

In addition to addressing the above questions, the data collected by the Sanitation Districts are merged into the Central Bight Cooperative Water Quality Survey (CBCWQS). These regionally coordinated surveys span over 200 kilometers of continuous coastline, between Ventura and Orange Counties, and contribute to understanding seasonal patterns in nearshore water column structure. These surveys are also contributed to the Santa Monica Bay Restoration Commission's Pelagic Ecosystem Monitoring program.

The MRP specifies the collection of continuous profiles of DO, temperature, salinity, light transmissivity (LT), chlorophyll-a (CHL), and pH from the surface to the bottom (or maximum depth of 100 m) at 48 sites on a quarterly basis. The MRP further specifies collection of samples for ammonia analysis from 24 of these sites at 0.5, 15, 30, and where possible, 45 m depths. The MRP also requires monthly measurement of the photosynthetic light energy at seven nearshore sites.

Throughout 2018 and 2019, JWPCP effluent was discharged through two continuously used outfalls off White Point on the Palos Verdes Peninsula. Hydraulic analysis predicts a 35:65 flow split between the 90-inch outfall, and the 120-inch outfall (Chapter 1, Figure 1.1). In the winter of 2019, the 72-inch outfall was also used from February 2 to February 3 for approximately 14 hours to provide hydraulic relief during high flows associated with heavy rain. All of the outfalls have extended diffusers to increase initial dilution of effluent with ambient seawater.

Using published United States Environmental Protection Agency models (Baumgartner et al. 1994), minimum initial dilutions for determining NPDES permit compliance with the COP have been calculated as 166:1 for the JWPCP discharge under static (zero current) conditions. The initial dilution process takes only minutes to form a highly dilute effluent plume which is advected and dispersed by ocean currents. Tidal (approximately semi-diurnal) and diurnal current reversals routinely dominate the energy spectra in the inner part of the Southern California Bight (SCB; Hendricks 1974, 1975; Winant and Bratkovitch 1981; Jones et al. 1986). The Sanitation Districts' measurements of currents on the Palos Verdes Shelf near the outfalls found typical current speeds were 9-15 cm/sec (LACSD 2008). Instantaneous currents of this speed significantly increase the predicted initial dilution of the effluent when incorporated into dilution models. The Sanitation Districts' measurements also found that net currents, after filtering out tidal and diurnal variability, are usually minimal in the cross-shelf direction. However, net speeds of along-shelf, coast-paralleling currents, were on average 4 cm/sec. Because along-shelf currents have coherence scales of greater than 25 km (Hendricks 1982, Winant 1983), they play an important role advecting effluent away from the discharge site. Typical net and average currents should advect the effluent plume 4-12 km or more away from the outfalls in one day.

Entrainment of ambient bottom water by the buoyant effluent is implicit in the initial dilution process. Trapping of the effluent plume below the surface occurs as the rising effluent plume reaches equilibrium in the density stratified water column. On average, the centerline of the plume is trapped approximately 30 m above the discharge depth, and 30 m below the surface. Dissolved oxygen (DO) concentrations and pH decrease with increasing depth, due to density stratification. Entrainment of this naturally stratified bottom water is unavoidable and must be accounted for in the assessment of these parameters for compliance determination.

### Chapter overview

This chapter provides results for the Nearshore/Offshore Water Quality Monitoring from 2018 and 2019. It describes the methodology used to collect and analyze water column data, describes and illustrates temporal and spatial trends and patterns, and assesses compliance with the NPDES permit limits.

This chapter is one component of the JWPCP Biennial Receiving Water Monitoring Report (LACSD 2020a). The complete report includes results and analyses for all JWPCP NPDES receiving water monitoring requirements and associated appendices. Electronic copies of the complete JWPCP Biennial Receiving Water Monitoring Report can be downloaded from the Sanitation Districts' website, www.lacsd.org.

### MATERIALS AND METHODS

### Field sampling

The Sanitation Districts monitor ocean conditions along the Palos Verdes Peninsula where outfalls discharge treated effluent from the JWPCP. Monitoring and reporting requirements are specified in the MRP (Appendix 1.1).

During quarterly offshore water quality surveys, the Sanitation Districts sampled a total of 48 sites (**Figure 2.1**). The Sanitation Districts' research vessel, *Ocean Sentinel*, is equipped with differential GPS to locate each sampling site. Vertical profiles of the water column were made at each site from the surface to the bottom, or to a maximum depth of 100 meters, using a conductivity, temperature, and depth (CTD)

instrument. The CTD includes probes for *in situ* measurement of pressure, temperature, conductivity, DO, pH, light transmissivity (LT), chlorophyll (CHL) and colored dissolved organic material (CDOM). All sensors scan the water 24 times per second. The CTD sends real time data to a deck unit and computer for storage. Detailed calibration and operating procedures are included in **Appendix 2.1**.

Discrete water samples were collected at 0.5, 15, 30, and where possible, 45 m depths at 24 sites. These samples were preserved and held on ice in the field until refrigeration was accessible at JWPCP. The laboratory SOP used for analysis of ammonia is included in **Appendix 2.2**.

Monthly measurements of light energy penetration were made at seven nearshore sites (nominal bottom depth of 18.3 m; **Figure 2.2**). Surveys were conducted on clear days, if possible, with minimal cloud cover between 10 a.m. and 2 p.m. The sites were located by differential GPS and confirmed with visual line-ups and fathometer readings. A submersible scalar irradiance sensor recorded photosynthetically active radiation (PAR) between 400 and 700 nanometer wavelengths at 0.5 m, 1 m, and 2 m depths, and thereafter every 2 meters until the bottom was reached. A hemispherical on deck unit simultaneously monitored incident irradiance above the surface for comparison. Surface temperature, Secchi disc depth, and water color (FOREL-ULE scale) were also measured during nearshore light energy surveys, and observations of wind, weather, swell, tides, and characteristics of the water (*e.g.* discoloration, turbidity, odor, and unusual or abnormal amounts of floating or suspended -debris) were recorded. More detailed field sampling procedures are described in Appendix 2.1.

### Data reduction

CTD data processing is a multi-step process, which takes the raw voltages and frequencies produced by the CTD sensors, and produces final electronic data files, tables and graphics of results in the appropriate engineering units. The data processing procedures follow the established guidelines of the CBCWQS group.

Using the sensor manufacturer's software package, SBE Data Processing, temperature and conductivity data were aligned, and compensations were processed for small delays
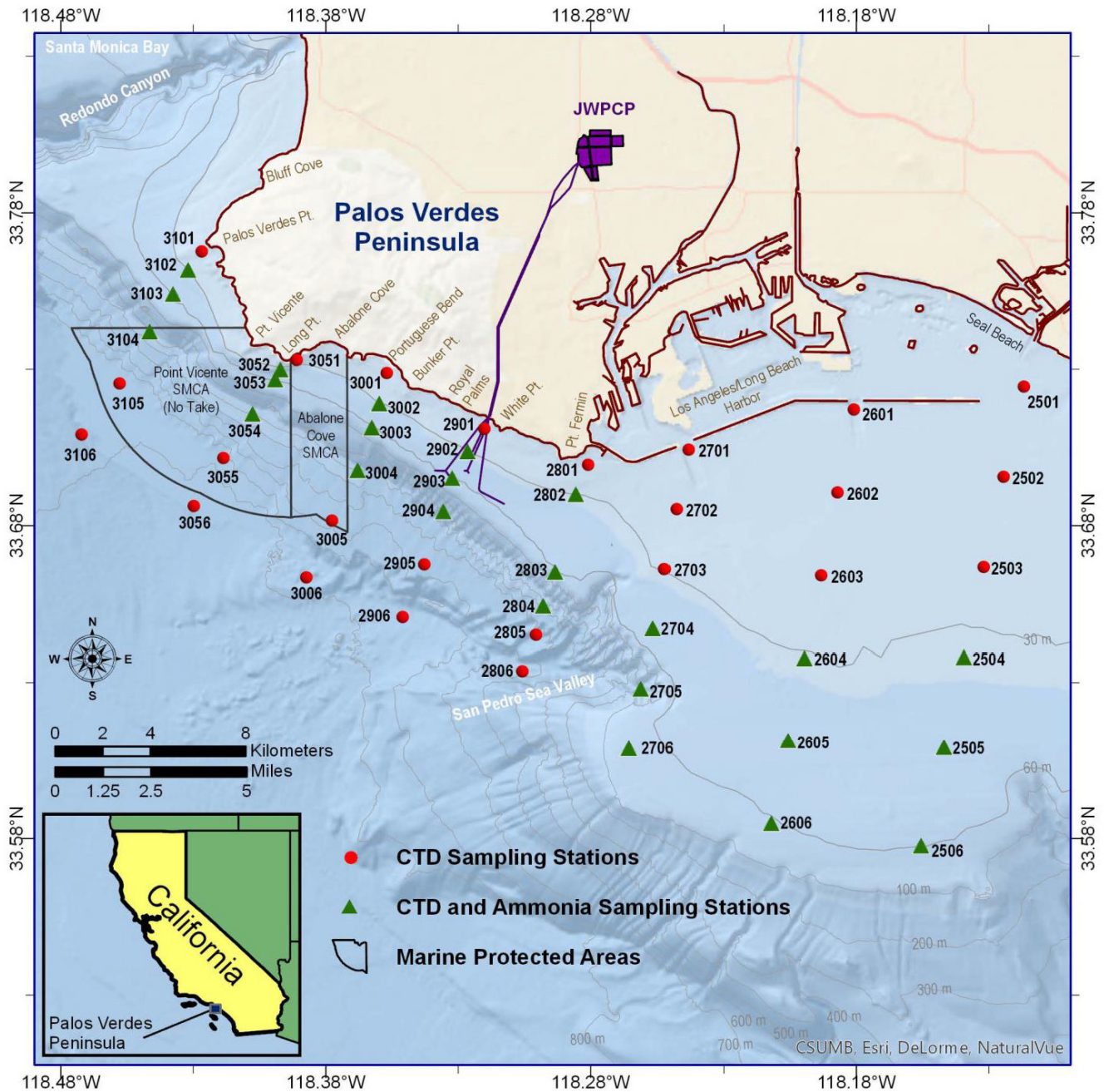
## Figure 2.1 Map of Offshore CTD Sampling Sites

Map of the Palos Verdes Peninsula and San Pedro shelf showing the positions of the 48 offshore sites sampled quarterly by the Sanitation Districts as part of the cooperative water column monitoring program. These sites are sampled for temperature, conductivity, salinity, density, dissolved oxygen, pH and chlorophyll-a fluorescence, from surface to bottom, or to 100m at deeper offshore stations. Discrete sampling for ammonia nitrogen is done at the surface, and 15, 30 and 45 meter depths at 24 of these sites (triangle sites).

introduced by water pumping across the sensors. After alignment, the individual downcast data for each parameter (temperature, salinity, DO, etc.) were checked. A minimal number of outlier data (<0.1%), almost all linked to trapped air bubbles at the surface, or interference when the CTD encounters the sea floor, were removed, but only when the value could not represent a real feature. After inspection, the downcast data were bin-averaged at one-meter depth intervals. Details of the procedures for data processing are included in Appendix 2.1.

Light energy survey measurements were recorded directly to a tablet using the Light

Energy application developed by the Sanitation Districts. The percentage of surface light energy reaching each depth was calculated using the ratio of light measured on the deck to the light measured at each depth, with all depth percentages based relative to the surface at 100%.

## Data analysis

Summary statistics of CTD parameters were compiled for discrete depth ranges in each quarter of 2018-2019. The CTD data were also used to produce three-dimensional (3D) spatial distribution patterns of DO, pH, LT, and CHL. Depth and seasonal variability in these parameters are described by referring to the 3D figures (**Figures 2.3-2.6**).

To assess COP compliance with DO, pH, and light transmissivity standards in the SCB, scientists at the Southern California Coastal Water Research Project (SCCWRP; Nezlin et al., 2016) developed an online software tool ([https://sccwrp.shinyapps.io/potw_compliance/](https://sccwrp.shinyapps.io/potw_compliance/)) in collaboration with most of the major Publicly Owned Treatment Works (POTW) dischargers in Southern California and staff from the State Water Resources Control Board. The tool accounts explicitly for the effects of entrainment and was applied independently during each quarterly survey in 2018 and 2019 to the data collected at the 48 offshore sites.

For each quarterly data set, the Plume and Reference sites were first identified (**Figure 2.7**). The plume was identified using the >95th percentile CDOM levels at sites within 8 km of the outfall, and at depths between 20 m below the surface and 10 m above the bottom. Reference sites were identified using the <85th percentile CDOM at sites up to 7 km from the outfall. At each Plume site, all depths with CDOM >95th percentile were assessed against Reference, using percent difference for oxygen or numeric difference for pH. Offshore Plume and Reference LT data were assessed for statistical difference by a one-tailed t-test. Because site 2903 is within the initial mixing zone (Zone of Initial Dilution, ZID), it is not subject to the compliance objectives.

Longer term discharge impacts on offshore waters were evaluated by comparison of annual averages of selected CTD water column parameters at 30 m (selected to represent an average plume trapping depth), at the ZID and a reference site, during the last 34 years. Levels of DO and pH were compared using time series plots, scatterplots, and plots of average seasonal cycles.

Temporal trends in nearshore light energy were evaluated using a 38-year data set of the average annual PAR reaching to 18 m from all sites. This was compared to the annual average PAR at 18 m at the sites nearest to the outfalls.

## RESULTS

All Nearshore/Offshore Water Quality monitoring and Nearshore Light Energy monitoring required by the MRP was completed in 2018 and 2019. A complete data set for the 2018 and 2019 surveys was submitted to the Los Angeles Regional Water Quality Control Board in August of 2019 and 2020, respectively (LACSD 2019a, LACSD 2020b). Additional supporting data for all Nearshore/Offshore Water Quality surveys for 2018 and 2019 is included in the appendices.

**Table 2.1** summarizes the results of the eight-quarterly offshore CTD surveys completed in 2018-2019. Average values of temperature, salinity, LT, DO, DO percent saturation, pH, CHL, and CDOM are provided for the discrete depth ranges of surface to 10 m, 11-30 m, 31-60 m, 61-100 m, and surface to 100 m. Average values for each year were also calculated, and minimum and maximum values of each parameter are reported for each survey and for the full year.

The lowest average temperature for the entire water column, 11.4 °C, occurred in May 2019. The highest average temperature, 16.0 °C, was seen in August 2018. Minimum and maximum temperatures in the survey area were 9.5 °C at 100 m depth in May 2018, and 24.8 °C at the surface in August 2018. For all of 2018 and 2019, the average temperature between 61 to 100 m was 11.5 °C and in the upper 10 m was 16.8 °C. This temperature difference creates the density structure that keeps the effluent trapped away from the surface.

The highest average salinity through the water column, 33.71 practical salinity units (psu), was seen in May 2019. The lowest average salinity, 33.47 psu, was recorded in February 2018. Discrete values of salinity ranged from a low of 32.72 psu in February
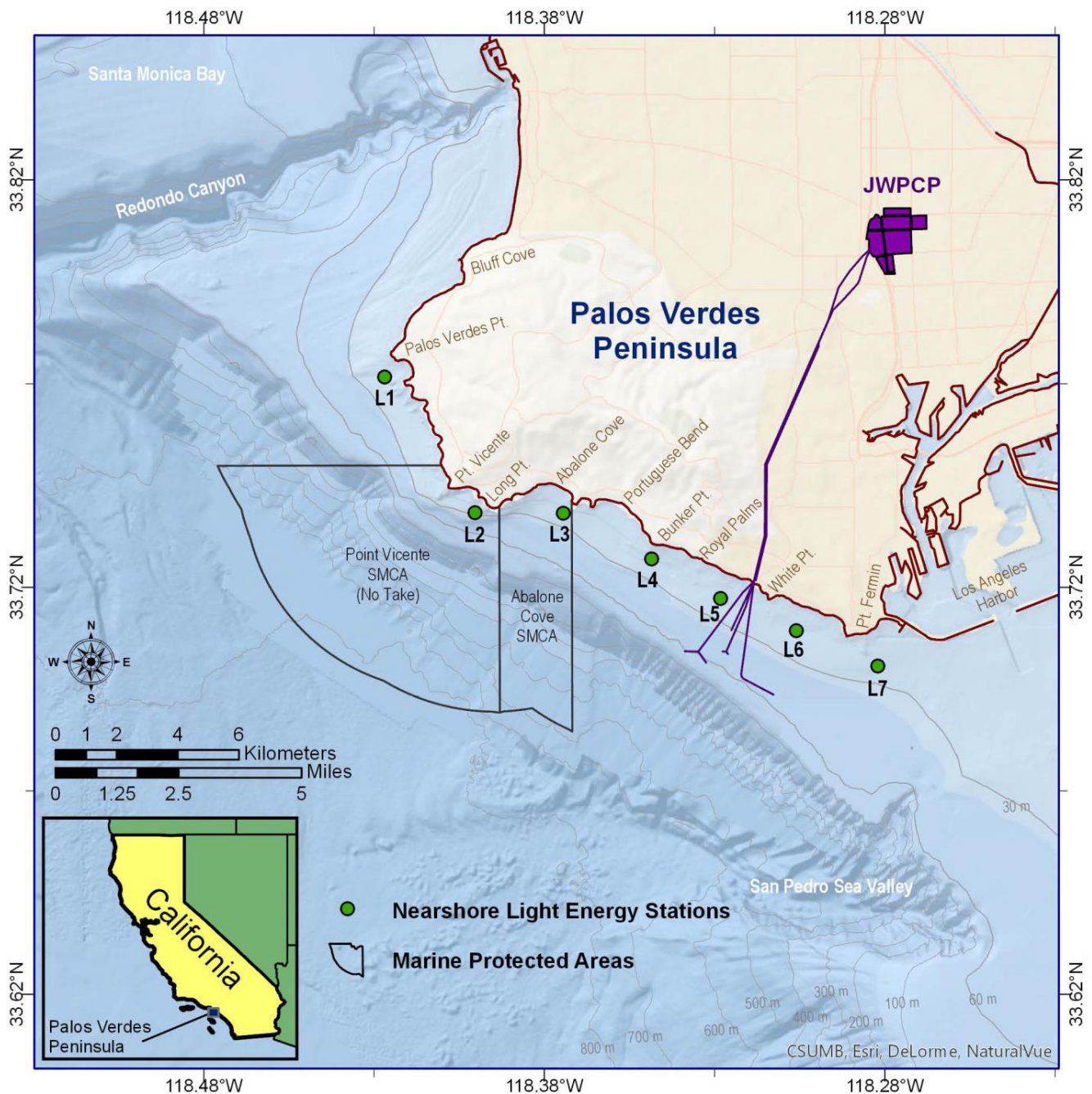
**Figure 2.2 Map of Nearshore Light Energy Monitoring Sites**
Map of the Palos Verdes Peninsula showing the seven nearshore sites sampled monthly for photosynthetically available light energy.

2019 to a high of 34.00 psu in May 2019. Reflecting the limited stratification in salinity, the 2018-2019 average salinity between 61 to 100 m was 33.60 psu, while the salinity in the top 10 m was 33.59 psu.
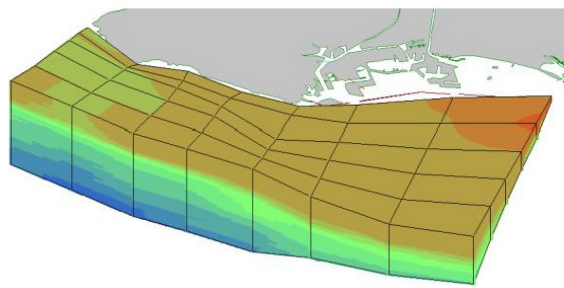
DO concentrations were variable through 2018-2019. Discrete values for all surveys ranged from 3.1 to 10.6 mg/L. The lowest average concentration through the upper 100 m of the water column was seen in May 2019, at 4.9 mg/L and was associated with spring season upwelling. The highest average concentration, 7.6 mg/L, was measured in February 2019. Reflecting the strong stratification in DO, the 2018-2019 average DO between 61 and 100 m was 5.2 mg/L while DO
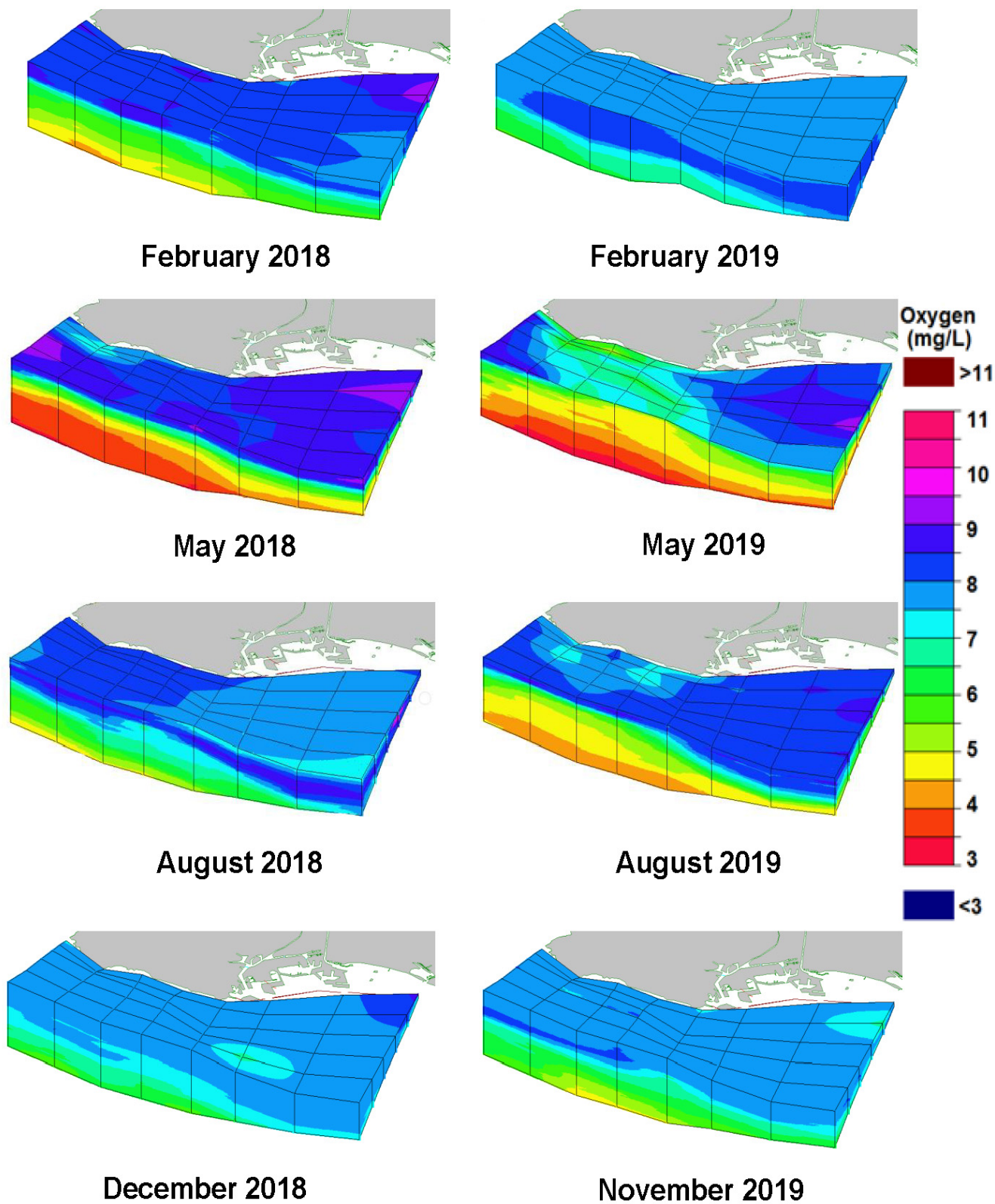
**Figure 2.3 3D Views of Dissolved Oxygen**

Dissolved oxygen (mg/l) 3D view showing surface patterns and offshore structure from the surface to 100m depth. The same color scale is used for each quarterly survey in 2018 and 2019. Note that the intersection of the grid lines on the plots correspond to the sampling sites shown in Figure 2.1.
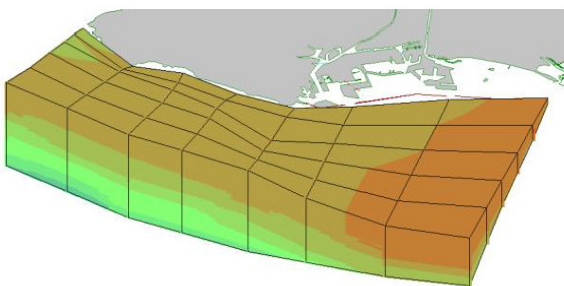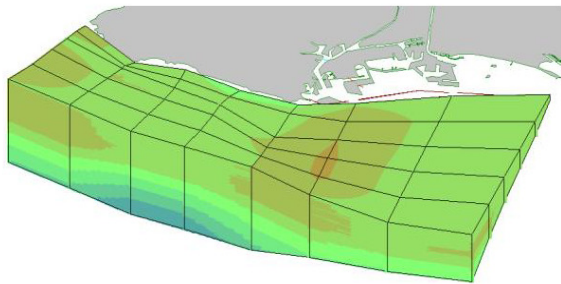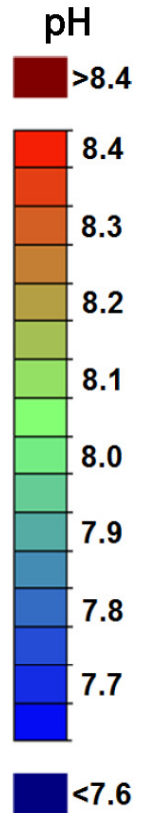
February 2018      February 2019

May 2018      May 2019
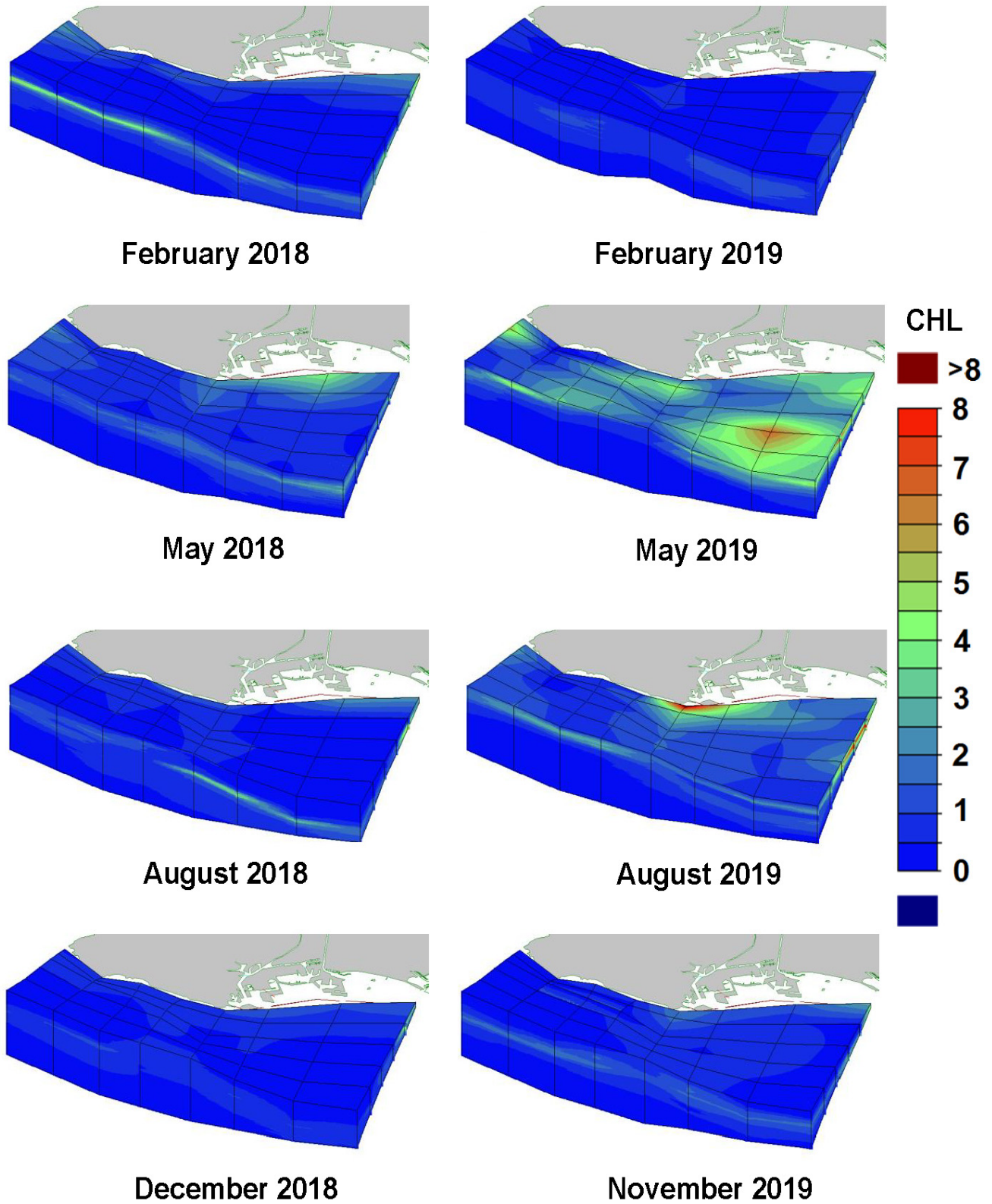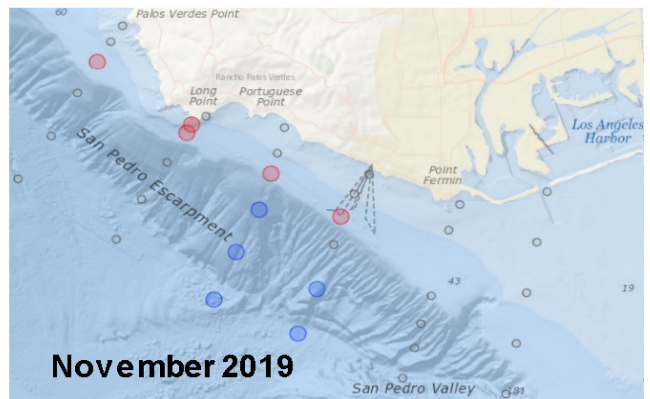
August 2018      August 2019

December 2018      November 2019

**pH**
>8.4
8.4
8.3
8.2
8.1
8.0
7.9
7.8
7.7
<7.6
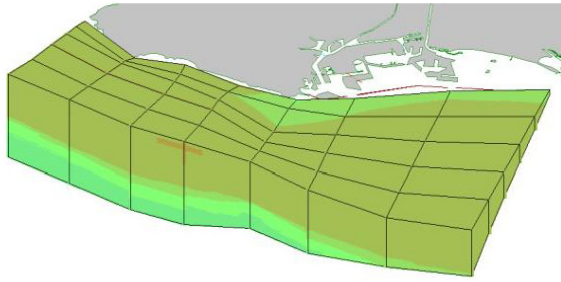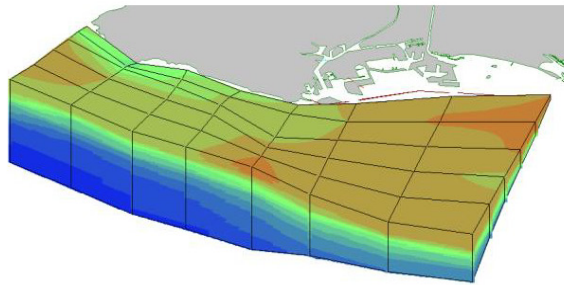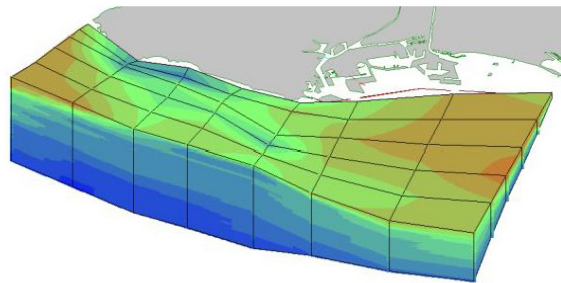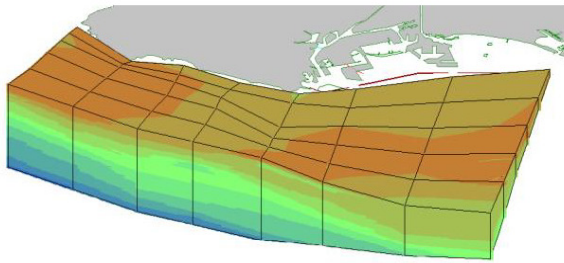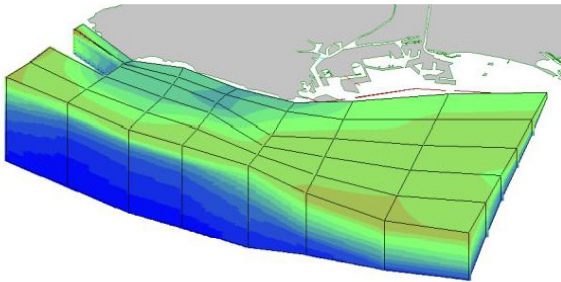
## Figure 2.4 3D Views of pH

pH 3D view showing surface patterns and offshore structure from the surface to 100m depth. The same color scale is used for each quarterly survey in 2018 and 2019. Note that the intersection of the grid lines on the plots correspond to the sampling sites shown in Figure 2.1.
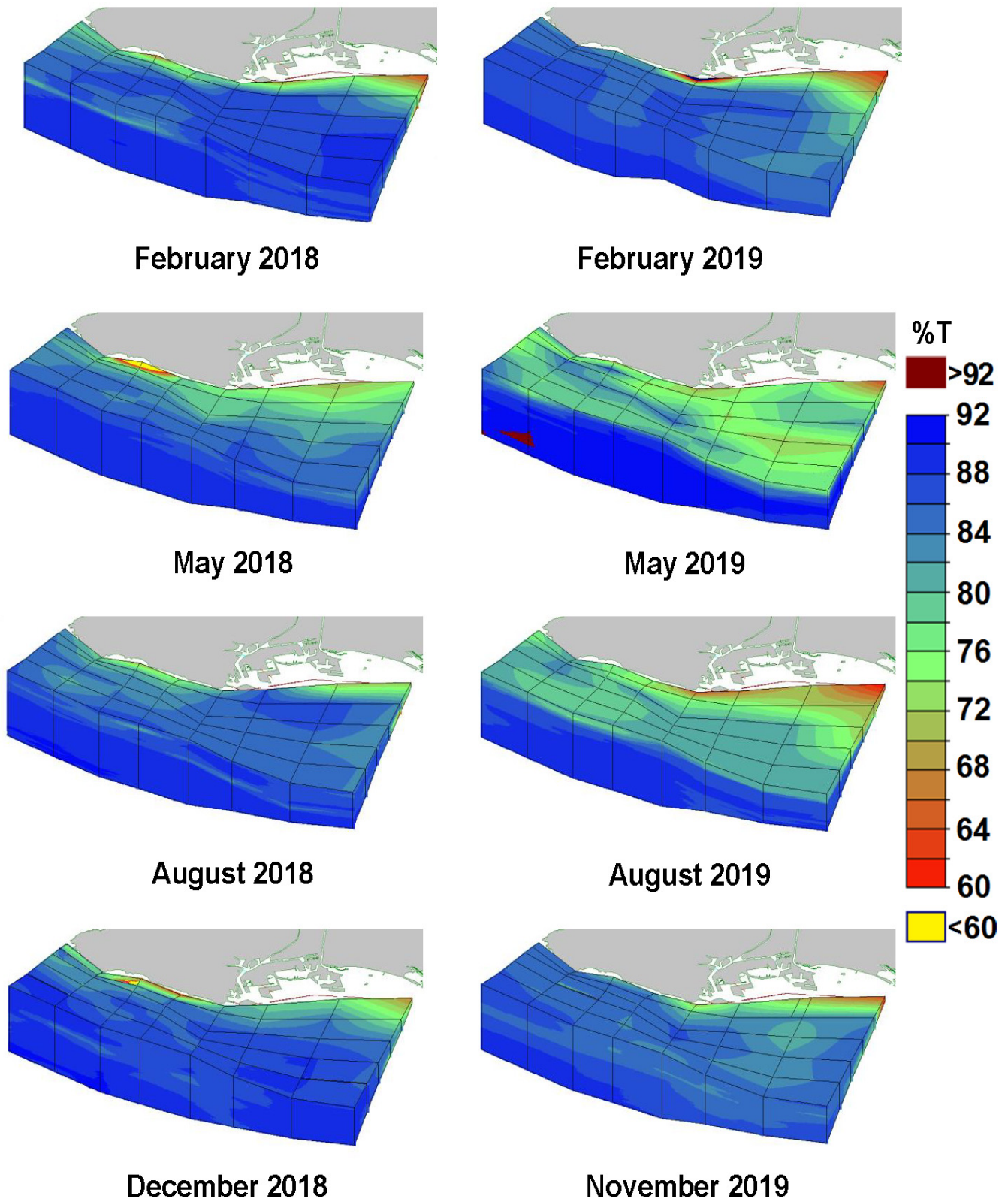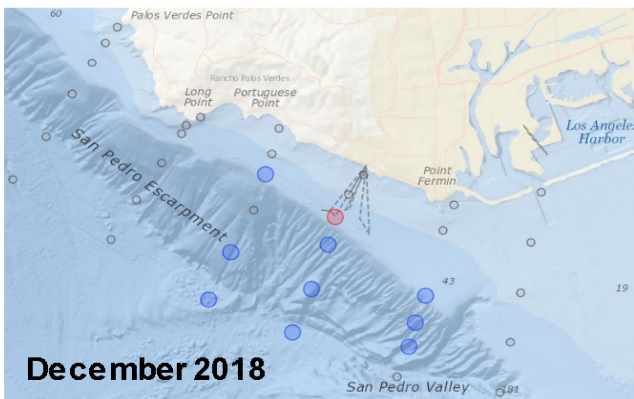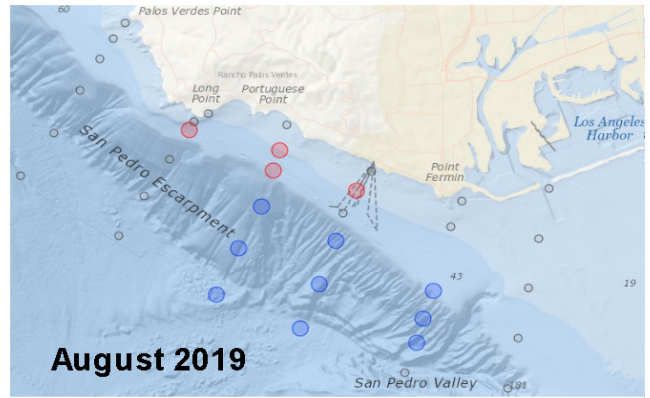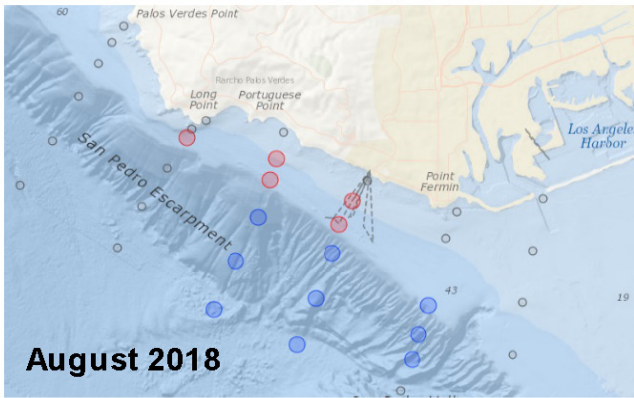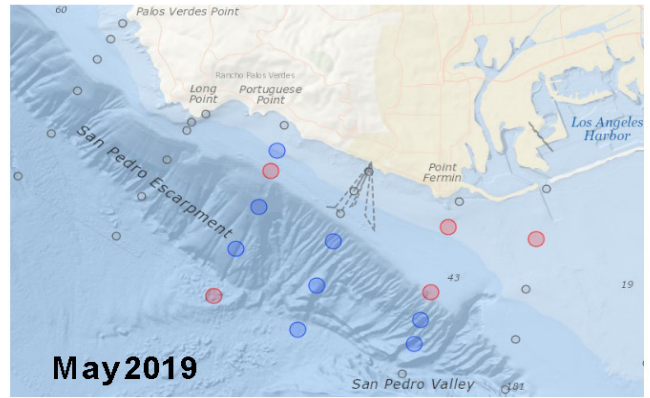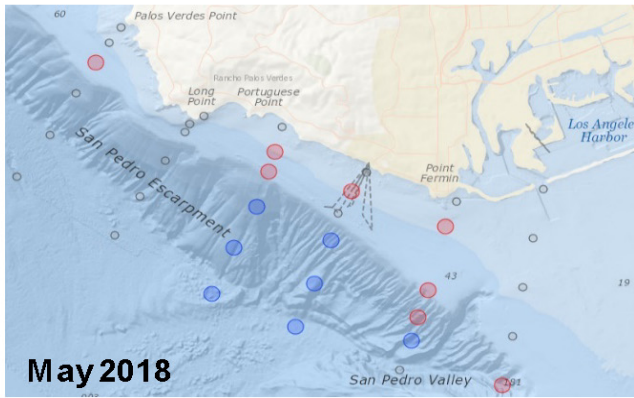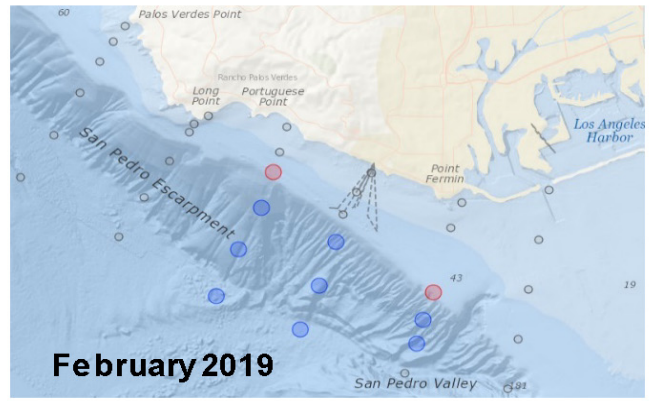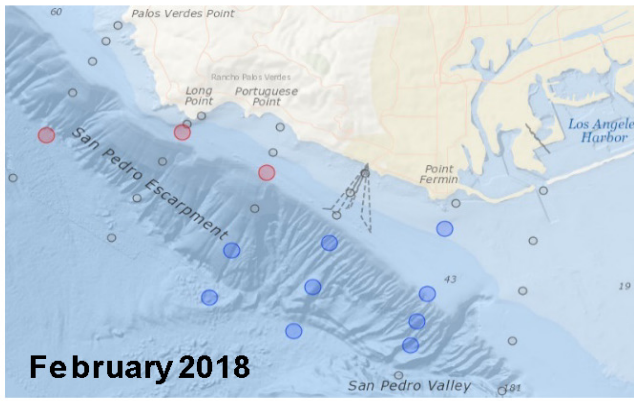
## Figure 2.5 3D Views of Light Transmission (LT)

LT 3D view showing surface patterns and offshore structure from the surface to 100m depth. The same color scale is used for each quarterly survey in 2018 and 2019. Note that the intersection of the grid lines on the plots correspond to the sampling sites shown in Figure 2.1.

**February 2018**

**February 2019**

**May 2018**

**May 2019**

**CHL**

>8
8
7
6
5
4
3
2
1
0

**August 2018**

**August 2019**

**December 2018**

**November 2019**

# Figure 2.6 3D Views of Chlorophyll-a Fluorescence (CHL)

CHL 3D view showing surface patterns and offshore structure from the surface to 100m depth. The same color scale is used for each quarterly survey in 2018 and 2019. Note that the intersection of the grid lines on the plots correspond to the sampling sites shown in Figure 2.1.

**February 2018** / **February 2019** / **May 2018** / **May 2019** / **August 2018** / **August 2019** / **December 2018** / **November 2019**

## Figure 2.7 Plume and Reference Sites

The compliance algorithm uses CDOM to identify Plume sites (red), and Reference sites (blue). Maps show locations of all Plume and Reference sites used for compliance assessment for each quarterly survey in 2018 and 2019. Note that the algorithm selects only a subset of depths at each site, not the entire water column.

in the top 10 m averaged 7.8 mg/L. The average DO saturation for the upper 100 m ranged from a low of 55% in May 2019, to 92% in August 2018 and February of 2019. Associated with spring upwelling, the lowest average DO saturations between 61 to 100 m, 41% and 42%, were recorded in May 2018 and May 2019, respectively. During all surveys in 2018 and 2019, discrete values of DO saturation ranged from 34% to 146%. Reflecting the importance of stratification on DO saturation, the 2018-2019 average DO saturation between 61 to 100 m was 60%, while DO saturation in the top 10 m averaged 98%.

The full range of discrete pH values in the upper 100 m for 2018-2019 was 7.6 to 8.3 pH units. The average pH between 61-100 m ranged from 7.7 to 8.0 pH units in 2018-2019, with the lowest average pH in this depth range observed in May 2018 and 2019, as well as August 2019. Reflecting the limited stratification in pH, the 2018-2019 average pH between 61-100 m was 7.9, while the pH in the top 10 m was 8.1.

For all surveys in 2018 and 2019, the majority of the sampled water was consistently clear. Overall average LT values for individual surveys ranged from 85.3% to 87.8%. Average LT in the upper 10 m of the water column, including data from the sites nearest to shore, ranged from 78.7% in August 2019 to 84.2% in December 2018. Offshore, at depths between 31-60 m, comparable to the discharge and mixing depth for the effluent, average LT ranged from 86.1% in November 2019 to 90.3% in May 2019.

For all surveys in 2018 and 2019 discrete values of CHL ranged from 0.1 µg/L to 9.8 µg/L. Average CHL values for the upper 100 m ranged from a low of 0.6 µg/L to 1.1 µg/L. Average levels of CHL in the upper 10 m were most variable, ranging from 0.6 µg/L in February 2019 to 2.6 µg/L in May 2019. Overall average CHL in the survey volume (surface to 100 m at all sites) ranged from 0.6 µg/L in December 2018 to 1.1 µg/L in February 2018. Peak CHL ranged from 1.6 µg/L in February 2019 to 9.8 µg/L in August 2019. Reflecting the vertical distribution of CHL, the 2018-2019 average concentration between 61-100 m was 0.3 µg/L, the concentration in the 11-30 m layer was 1.3 µg/L, and the concentration in the top 10 m was 1.3 µg/L.

Average CDOM values for the upper 100 m ranged from 0.49 µg/L in February 2019 to 0.90 µg/L in November 2019. CDOM is an effective indicator of the effluent, and at sites and depths where the effluent field was present, CDOM was measured at up to several times background levels and as high as 3.55 µg/L.

Tabular summaries of all ammonia results collected in 2018-2019 are included in **Appendix 2.3**. Ammonia above the Reporting Level (RL) of 0.02 mg/L was detected in 205 of 716 samples collected in 2018-2019. An additional 300 samples had detected ammonia at levels between the RL and the Method Detection Level (MDL) of 0.003 mg/L. In this range the ammonia concentration was estimated, and the results are considered to indicate that ammonia was present, but not quantifiable. The remaining 211 samples had no detectable ammonia, meaning that levels were below the MDL. The maximum ammonia concentration in 2018-2019 was 0.43 mg/L, measured at the 45 m depth at site 2903, located within the ZID, in August 2018. Only 12% of surface samples had detected ammonia, with values ranging from 0.02 to 0.12 mg/L. At 15 m, 39% of samples had ammonia, and detected values ranged from 0.02 to 0.26 mg/L. At 30 m, 32% of samples had ammonia, and the detected values ranged from 0.02 to 0.33 mg/L. At 45 m, 27% of samples had ammonia and detected values ranged from 0.02 to 0.43 mg/L.

Tabular summaries of all required visual observations recorded during quarterly offshore sampling in 2018-2019 are included in **Appendix 2.4.**

The percentage of PAR light energy reaching 18 m at each of the nearshore sites during 2018 and 2019 is reported in **Table 2.2**. The overall average light energy reaching the 18 m nominal bottom depth for all sites and months in 2018-2019 was 2.84%. Reflecting the great variability in nearshore conditions, light energy at 18 m ranged from a low of 0.11% at site L4 in December 2018, to a high of 11.29% at site L2 in November 2018. In 2018, average 18 m light energy for all sites ranged from 0.63% in December to 7.33% in November. In 2019, average 18 m light energy ranged from 1.06% in June to 4.49% in August. Variability in the annual average light energy between sites was more limited. In 2018, average light energy at 18 m ranged from

# Table 2.1 Coastal Water Quality Summary Statistics

Average values of selected CTD parameters over varying depth ranges. Annual average and full depth range averages in **bold**.

| Variable | Depth Range (Meters) Min | Max | 2018 Feb | May | Aug | Dec | Avg | 2019 Feb | May | Aug | Nov | Avg |
|---|---|---|---|---|---|---|---|---|---|---|---|---|
| Temperature | 1 | 10 | 15.6 | 14.9 | 22.6 | 16.8 | **17.5** | 15.3 | 13.7 | 17.1 | 17.9 | **16.0** |
| (Deg. C) | 11 | 30 | 15.0 | 12.6 | 17.8 | 16.7 | **15.5** | 15.3 | 11.7 | 13.1 | 16.9 | **14.2** |
| | 31 | 60 | 13.0 | 10.5 | 13.8 | 15.6 | **13.2** | 15.0 | 10.8 | 11.4 | 13.9 | **12.8** |
| | 61 | 100 | 11.4 | 9.8 | 11.8 | 13.2 | **11.5** | 13.2 | 10.0 | 10.6 | 12.2 | **11.5** |
| | **1** | **100** | **13.7** | **11.7** | **16.0** | **15.5** | **14.2** | **14.7** | **11.4** | **12.7** | **15.0** | **13.4** |
| *Minimum Individual Measurement* | | | 10.6 | 9.5 | 10.3 | 11.3 | **10.4** | 11.9 | 9.7 | 10.0 | 11.1 | **10.7** |
| *Maximum Individual Measurement* | | | 16.9 | 17.0 | 24.8 | 17.4 | **19.0** | 15.6 | 17.0 | 21.1 | 18.6 | **18.1** |
| Salinity | 1 | 10 | 33.48 | 33.58 | 33.73 | 33.55 | **33.58** | 33.56 | 33.61 | 33.62 | 33.61 | **33.60** |
| (ppt) | 11 | 30 | 33.46 | 33.56 | 33.58 | 33.60 | **33.55** | 33.60 | 33.64 | 33.55 | 33.57 | **33.59** |
| | 31 | 60 | 33.41 | 33.68 | 33.51 | 33.57 | **33.54** | 33.61 | 33.73 | 33.63 | 33.50 | **33.62** |
| | 61 | 100 | 33.54 | 33.87 | 33.58 | 33.56 | **33.64** | 33.58 | 33.87 | 33.74 | 33.63 | **33.71** |
| | **1** | **100** | **33.47** | **33.68** | **33.59** | **33.57** | **33.58** | **33.59** | **33.71** | **33.63** | **33.57** | **33.63** |
| *Minimum Individual Measurement* | | | 33.26 | 33.47 | 33.21 | 32.94 | **33.22** | 32.72 | 33.45 | 33.40 | 33.29 | **33.22** |
| *Maximum Individual Measurement* | | | 33.66 | 33.97 | 33.83 | 33.69 | **33.78** | 33.65 | 34.00 | 33.83 | 33.79 | **33.82** |
| Light | 1 | 10 | 83.8 | 82.4 | 83.6 | 84.2 | **83.5** | 83.5 | 80.2 | 78.7 | 83.4 | **81.4** |
| Transmittance | 11 | 30 | 84.1 | 86.2 | 84.7 | 85.1 | **85.0** | 85.2 | 87.4 | 84.9 | 83.3 | **85.2** |
| (%) | 31 | 60 | 87.3 | 88.8 | 88.2 | 86.7 | **87.8** | 86.8 | 90.3 | 88.1 | 86.1 | **87.8** |
| | 61 | 100 | 89.1 | 89.1 | 89.6 | 88.6 | **89.1** | 88.3 | 91.4 | 88.7 | 87.9 | **89.1** |
| | **1** | **100** | **86.1** | **87.0** | **86.7** | **86.3** | **86.5** | **86.0** | **87.8** | **85.7** | **85.3** | **86.2** |
| *Minimum Individual Measurement* | | | 62.4 | 34.1 | 61.7 | 36.0 | **48.5** | 46.1 | 62.4 | 59.5 | 59.8 | **56.9** |
| *Maximum Individual Measurement* | | | 90.1 | 90.0 | 90.4 | 90.3 | **90.2** | 89.2 | 92.2 | 89.6 | 88.7 | **89.9** |
| Dissolved | 1 | 10 | 8.3 | 8.1 | 8.0 | 7.7 | **8.0** | 7.9 | 6.5 | 7.7 | 7.8 | **7.5** |
| Oxygen | 11 | 30 | 7.8 | 6.3 | 8.2 | 7.7 | **7.5** | 8.0 | 5.0 | 6.4 | 7.7 | **6.8** |
| (mg/L) | 31 | 60 | 6.2 | 4.5 | 7.5 | 7.5 | **6.4** | 7.8 | 4.5 | 5.3 | 6.9 | **6.1** |
| | 61 | 100 | 5.1 | 3.7 | 5.8 | 6.6 | **5.3** | 6.7 | 3.8 | 4.6 | 5.6 | **5.2** |
| | **1** | **100** | **6.8** | **5.4** | **7.3** | **7.4** | **6.7** | **7.6** | **4.9** | **5.8** | **7.0** | **6.3** |
| *Minimum Individual Measurement* | | | 4.3 | 3.4 | 4.6 | 5.5 | **4.4** | 5.8 | 3.1 | 4.1 | 4.2 | **4.3** |
| *Maximum Individual Measurement* | | | 9.4 | 9.4 | 10.6 | 8.6 | **9.5** | 8.2 | 9.3 | 9.1 | 8.3 | **8.7** |
| pH | 1 | 10 | 8.2 | 8.1 | 8.2 | 8.2 | **8.2** | 8.1 | 8.0 | 8.0 | 8.1 | **8.1** |
| (pH units) | 11 | 30 | 8.1 | 8.0 | 8.1 | 8.2 | **8.1** | 8.1 | 7.9 | 7.9 | 8.1 | **8.0** |
| | 31 | 60 | 8.0 | 7.8 | 8.0 | 8.1 | **8.0** | 8.1 | 7.8 | 7.8 | 8.1 | **7.9** |
| | 61 | 100 | 7.9 | 7.7 | 7.9 | 8.0 | **7.9** | 8.0 | 7.7 | 7.7 | 8.0 | **7.8** |
| | **1** | **100** | **8.0** | **7.9** | **8.1** | **8.1** | **8.0** | **8.1** | **7.8** | **7.8** | **8.1** | **8.0** |
| *Minimum Individual Measurement* | | | 7.8 | 7.7 | 7.8 | 7.9 | **7.8** | 7.9 | 7.7 | 7.6 | 7.8 | **7.8** |
| *Maximum Individual Measurement* | | | 8.3 | 8.2 | 8.3 | 8.3 | **8.3** | 8.2 | 8.2 | 8.2 | 8.2 | **8.2** |
| Dissolved | 1 | 10 | 102 | 99 | 113 | 98 | **103** | 97 | 78 | 98 | 100 | **93** |
| Oxygen | 11 | 30 | 95 | 73 | 106 | 97 | **93** | 98 | 57 | 76 | 97 | **82** |
| Saturation | 31 | 60 | 73 | 50 | 89 | 92 | **76** | 95 | 50 | 60 | 83 | **72** |
| (%) | 61 | 100 | 57 | 41 | 66 | 78 | **61** | 78 | 42 | 51 | 65 | **59** |
| | **1** | **100** | **81** | **63** | **92** | **91** | **82** | **92** | **55** | **69** | **85** | **75** |
| *Minimum Individual Measurement* | | | 48 | 37 | 51 | 62 | **49** | 67 | 34 | 46 | 47 | **48** |
| *Maximum Individual Measurement* | | | 117 | 116 | 146 | 108 | **122** | 101 | 114 | 118 | 106 | **110** |
| *Chlorophyll* | 1 | 10 | 1.0 | 1.4 | 1.0 | 0.7 | **1.0** | 0.6 | 2.6 | 2.2 | 0.8 | **1.5** |
| Fluorescence | 11 | 30 | 1.9 | 1.5 | 1.3 | 0.8 | **1.4** | 1.0 | 1.2 | 1.4 | 1.3 | **1.2** |
| (ug/L) | 31 | 60 | 1.1 | 0.6 | 1.0 | 0.7 | **0.8** | 0.7 | 0.3 | 0.4 | 0.8 | **0.6** |
| | 61 | 100 | 0.3 | 0.2 | 0.4 | 0.3 | **0.3** | 0.3 | 0.2 | 0.2 | 0.3 | **0.2** |
| | **1** | **100** | **1.1** | **0.9** | **0.9** | **0.6** | **0.9** | **0.7** | **1.0** | **0.9** | **0.8** | **0.8** |
| *Minimum Individual Measurement* | | | 0.1 | 0.1 | 0.1 | 0.1 | **0.1** | 0.1 | 0.1 | 0.1 | 0.1 | **0.1** |
| *Maximum Individual Measurement* | | | 5.3 | 5.7 | 5.2 | 5.3 | **5.4** | 1.6 | 7.9 | 9.8 | 4.3 | **5.9** |
| *CDOM* | 1 | 10 | 0.61 | 0.77 | 0.55 | 0.50 | **0.61** | 0.50 | 0.71 | 0.60 | 0.77 | **0.64** |
| (ug/L) | 11 | 30 | 0.75 | 0.90 | 0.84 | 0.46 | **0.74** | 0.43 | 0.72 | 0.72 | 0.86 | **0.68** |
| | 31 | 60 | 1.06 | 0.93 | 0.95 | 0.63 | **0.89** | 0.44 | 0.60 | 0.62 | 0.99 | **0.66** |
| | 61 | 100 | 0.87 | 0.91 | 0.71 | 0.64 | **0.78** | 0.61 | 0.60 | 0.59 | 0.91 | **0.68** |
| | **1** | **100** | **0.84** | **0.89** | **0.78** | **0.56** | **0.77** | **0.49** | **0.66** | **0.64** | **0.90** | **0.67** |
| *Minimum Individual Measurement* | | | 0.28 | 0.48 | 0.09 | 0.18 | **0.26** | 0.25 | 0.37 | 0.21 | 0.56 | **0.35** |
| *Maximum Individual Measurement* | | | 2.47 | 1.90 | 3.55 | 1.63 | **2.39** | 1.80 | 1.57 | 1.61 | 2.67 | **1.91** |

2.30% at site L3, to 4.24% at site L7, and in 2019 average light energy at 18 m ranged from 1.88% at site L7, to 2.93% at site L3.

Field data summaries, for every month in 2018 and 2019, with all recorded light energy data, as well as measures of other water quality parameters, sea conditions, and weather, are included in **Appendix 2.5.**

# DISCUSSION

## Spatial and seasonal patterns, 2018-2019

Several of the parameters sampled by CTD have spatial patterns that vary by geographical location within the survey area, such as distance from the shoreline, or from a point source, such as a river outlet. Other parameters are depth stratified and routinely have greater variability over 100 m of depth than over the 33 kilometer range from one end of the survey area to the other. The effluent plume produces localized features in the distribution of some CTD parameters, but apart from ammonia and CDOM, the effluent plume effects on other measured parameters are generally far less than the natural variability.

Distributions of parameters that are depth stratified are determined by the vertical density structure, and density in the coastal waters is primarily a function of temperature with salinity being a secondary contributor. The greater the density stratification, the more restricted the vertical movement of chemical and biological parameters. Seasonal cycles of warming and cooling of the upper water column are most critical to the formation and structure of the vertical density regime.

In Southern California coastal waters, strong thermoclines form during the summer and remain in place until late fall (Winant and Bratkovich 1981). This cycle is routinely observed in the surveys off Palos Verdes. In contrast, in most years, several strong upwelling events are observed during the winter and spring months. During these events, the upper water column is cooled, and density stratification may be temporarily reduced or eliminated. Because of the unusual shelf topography, upwelling near Palos Verdes can be very localized, in which case temperature stratification may be reduced at just

a subset of sites, and the thermocline reforms rapidly when upwelling ceases.

The spatial patterns of key water quality parameters observed during 2018 and 2019 are discussed below. Graphics showing overlays of all 48 profiles in each quarter for most CTD parameters are included in **Appendix 2.6**. In addition to showing the range of values sampled, these plots include a depth–weighted mean profile to show the central trend of the data and highlight the profile from the ZID site. Depth weighted average profiles for eight parameters showing vertical distribution patterns for each quarter in 2018 and 2019 are shown in **Appendix 2.7**, and 3D views of each parameter in each quarter of 2018 and 2019 are shown in **Appendix 2.8**. The cycle of oceanographic conditions through the 2018 and 2019 calendar years was generally typical of previous years and was comparable between 2018 and 2019.

### Temperature

Daily measurements at JWPCP document that the effluent temperature at discharge ranges from 23 °C to 32 °C during the year. The ocean water temperature at the 30 to 60 meter depth of the outfalls generally ranges between 10 °C and 15 °C. After initial dilution, the typical expected change in ambient temperature at the edge of the ZID due to the discharge is approximately 0.1 °C. Due to the entrainment phenomena (described in the introduction), a slight upward deflection of cooler temperature isotherms is sometimes observed near the outfalls.

The seasonal range of natural temperature variability far exceeds the very small effect from the effluent discharge, while the natural variability in density determines the trapping depth and to some extent the initial dilution achieved by the discharged effluent. The average temperature in the upper 10m of the water ranged from 13.7 °C in May 2019 to 22.6 °C in August 2018 (Table 2.1). By comparison, seasonal cycles are reduced at depth. Average temperature between 61 and 100 m ranged from 9.8 °C in May 2018 to 13.2 °C in December 2018 and February 2019.

Summer (August) surveys regularly have the greatest thermal stratification. Although not as noticeable in averages, typical summer warming of the upper water column creates

## Table 2.2 Percent Light Energy at 18m, 2018-2019

The percent of light energy reaching 18 m at nearshore stations is shown for all monthly surveys made in 2018 and 2019. Levels of less than 1% are highlighted in bold red. *used 16 m result because 18 m depth not sampled

|  | | L1 | L2 | L3 | L4 | L5 | L6 | L7 | Average |
|---|---|---|---|---|---|---|---|---|---|
| **2018** | | | | | | | | | |
| | Jan | 0.80 | 1.45 | 1.95 | 0.43 | 2.55 | 3.19 | 2.95 | 1.90 |
| | Feb | 5.74 | 4.23 | 2.58 | 4.23 | 3.82 | 3.63 | 1.96 | 3.74 |
| | Mar | 3.45 | 5.60 | 3.63 | 3.25 | 4.29 | 4.19 | 4.15 | 4.08 |
| | Apr | 2.69 | 3.61 | 2.86 | 3.15 | 4.49 | 4.65 | 5.31 | 3.82 |
| | May | 1.26 | 4.09 | 1.74 | 1.88* | 2.40 | 3.56 | 4.42 | 2.77 |
| | Jun | 2.77 | 2.25 | 1.11 | 2.49* | 3.16 | 1.61 | 1.76 | 2.16 |
| | Jul | 0.63 | 1.48 | 2.17 | 1.51 | 2.30 | 2.61 | 7.89 | 2.65 |
| | Aug | 1.44 | 2.35 | 1.74 | 2.08* | 1.60 | 1.71 | 1.40 | 1.76 |
| | Sep | 0.78 | 3.08 | 2.74 | 3.53 | 2.56 | 3.00 | 3.19 | 2.70 |
| | Oct | 3.06 | 3.38 | 2.04 | 1.62 | 6.57 | 4.86 | 8.77 | 4.33 |
| | Nov | 10.4 | 11.3 | 4.12 | 3.88 | 6.32 | 7.07 | 8.26 | 7.33 |
| | Dec | 0.14 | 1.11 | 0.88 | 0.11 | 0.63 | 0.64 | 0.87 | 0.63 |
| **Average** | | 2.76 | 3.66 | 2.3 | 2.35 | 3.39 | 3.39 | 4.24 | 3.16 |
| | | | | | | | | | |
| **2019** | | | | | | | | | |
| | Jan | 2.06 | 2.09 | 1.76 | 1.96 | 2.46 | 3.04 | 1.03 | 2.06 |
| | Feb | 3.28 | 4.91 | 5.45 | 2.25 | 2.43 | 3.13 | 2.11 | 3.37 |
| | Mar | 2.47 | 4.05 | 1.30 | 3.31* | 2.43 | 1.43 | 2.33 | 2.48 |
| | Apr | 4.58 | 5.75 | 7.24* | 7.14* | 5.37 | 3.23 | 2.08 | 4.26 |
| | May | 1.72 | 1.58 | 3.18* | 0.42* | 0.33 | 0.53 | 0.74 | 1.21 |
| | Jun | 1.29 | 2.39 | 0.95 | 1.31 | 0.57 | 0.63 | 0.30 | 1.06 |
| | Jul | 4.20 | 4.53 | 2.66 | 3.58 | 2.73 | 1.79 | 0.75 | 2.89 |
| | Aug | 2.45 | 3.75 | 4.76 | 3.82 | 4.49 | 6.07 | 6.06 | 4.49 |
| | Sep | 2.79 | 2.61 | 2.11 | 1.48 | 1.43 | 0.83 | 1.62 | 1.84 |
| | Oct | 2.16 | 1.55 | 1.43 | 1.16 | 1.51 | 1.91 | 1.31 | 1.58 |
| | Nov | 2.56 | 3.05 | 2.67 | 3.13 | 3.22 | 2.50 | 2.50 | 2.80 |
| | Dec | 4.38 | 2.59 | 1.61 | 1.38* | 1.00 | 1.71 | 1.74 | 2.06 |
| **Average** | | 2.83 | 2.77 | 2.93 | 2.58 | 2.33 | 2.23 | 1.88 | 2.51 |

differences in temperature up to 10°C at many sites between the surface and the 60 m depth (Appendix 2.6). Extreme warm temperatures occur near the surface during summer. In August 2018 and August 2019, average maximum temperatures were at the surface and were 22.6 °C and 17.1°C, respectively, while average minimum temperatures found at 100 m depths were 11.8 °C and 10.6 °C, respectively (Table 2.1). The stratified conditions seen in summer surveys are generally maintained into the fall, even as near surface temperatures begin to drop, although this was not the case in 2019.

In fall (December 2018, November 2019), with fewer daylight hours and less direct sun, surface temperatures tend to drop, and the thermocline moves deeper. However, the average

temperature for the upper 100 m does not decline significantly from summer, and in the case of November 2019 continued to increase.

Upwelling conditions were observed in spring (May) of 2018 and 2019 in response to offshore winds that are most active in winter and spring. In each of these quarters, the upwelling was confirmed by deep offshore (100 m depth) minimum temperatures at or below 10° C and higher salinities than in other quarters.

*Salinity*

The freshwater effluent discharge reaches the ocean where average salinity at 31 to 60 meters ranges from 33.4 to 33.7 psu (Table 2.1). After initial dilution, the expected reduction in

salinity at the edge of the ZID is approximately 0.2 psu, about equal to the average natural seasonal variability of salinity in ocean waters. The observed reduction of salinity in the effluent plume can be less than expected, because as it rises, the plume entrains ambient water with higher salinity than the ambient background at the trapping depth. Nonetheless, reduced salinity can generally be used to identify the effluent plume at sites near the outfalls; at greater distances, the salinity signal is lost in the background variability.

A secondary phenomenon associated with the annual cycle of temperature-dominated density stratification is the appearance of a salinity minimum layer. Typically, salinity increases with depth in the ocean. However, in coastal waters off Southern California, the vertical salinity structure can become inverted. In summer and fall, when a strong thermocline is present, warm near-surface water increases in salinity due to evaporation. Because of its higher temperature, it remains less dense than the slightly less saline water below the thermocline. This results in the formation of a sub-surface layer of lower salinity. Jones et al. (2002) identified this feature from hydrographic surveys over the Palos Verdes shelf. Dorman and Palmer (1981) describe a salinity minimum layer in the California Current at about 100 m depth swinging east (towards the Southern California coastline), and advected around the SCB at 30 to 50 m in depth.

The summer and fall (August 2018 & 2019, November 2019) average salinity profiles for 2018 and 2019 (Appendix 2.7) show this feature clearly. Because the effluent plumes from the major ocean dischargers are typically trapped below the thermocline, they generally overlap the same depth range where the natural salinity-minimum feature is located, and it can appear that the reduced salinity is direct evidence of the effluent plume. However, review of years of CBCWQS salinity data confirms that the sub-surface salinity feature is observed over the entire regional survey area, including locations far removed from effluent discharges.

*Dissolved oxygen*

Direct DO reduction of the receiving waters due to the biological oxygen demand (BOD) of effluent is a key concern of dischargers and regulators. A secondary concern is that nutrients in the effluent may stimulate excessive phytoplankton growth (eutrophication), which may cause oxygen reductions if the excess phytoplankton dies and decomposes. During 2018-2019, daily samples of JWPCP final effluent BOD ranged from 3.5 to 7.7 mg/L, with an average of 4.6 mg/L, a 99% decrease from the average influent BOD of 437 mg/L (LACSD 2019b, 2020c). After initial dilution the DO reduction in receiving water due to effluent BOD should be less than 0.03 mg/L, or about 1% of the average DO levels in the receiving water. Since JWPCP BOD is measured over a five-day period, but the effluent reaches the boundary of the ZID within minutes, this estimate is very conservative.

DO distributions are primarily associated with vertical density stratification. Figure 2.3 shows the patterns of DO in each quarter of 2018-2019. These graphics plot the data sampled at CTD sites on the offshore outer edge and eastern cross-shelf edge of the survey area, together with the DO surface distributions from all 48 CTD sites. Surface DO distributions over the survey area are variable, and do not reveal any regular spatial patterns. Average DO concentrations in the upper 10 m of the water column ranged from 6.5 to 8.3 mg/L (Table 2.1). Due to wave and current mixing, DO concentrations in surface waters are generally close to saturation. In the top 10 m, average percent saturation levels for all the quarters in 2018 –2019 ranged from 78% to 113%. When phytoplankton are present, surface and near surface waters may become supersaturated. Supersaturation was observed in all eight quarters of 2018 and 2019. Maximum discrete saturation levels in each quarter ranged from 101% to 146% (Table 2.1).

As depth increases, particularly below the thermocline, DO concentrations and percent saturation quickly decrease, reflecting the depletion of oxygen that occurs due to respiratory processes when water is trapped by density stratification away from the air-water interface. The lowest DO concentrations are routinely seen at the deepest sampling points and often associated with spring season upwelling when the deepest water is moved upward. The lowest annual measured DO concentrations, in May 2018 and May 2019, were 3.4 and 3.1 mg/L, respectively. The combined average of DO concentrations between 61-100 m in these two quarters was 3.8 mg/L, 34% lower than during other times of year when DO between these

depths averaged 5.7 mg/L. Average percent saturation was also reduced, from 66% down to 41%, in these deepest sampled waters during the quarters when upwelling was active. Upwelling processes also had a comparable effect on waters in the 31 to 60 m layer where the outfalls discharge, and where the dilute effluent plume is usually observed. DO concentrations between 31 to 60 m during upwelling averaged 4.5 mg/L, 34% lower than non-upwelling concentrations of 6.9 mg/L. By comparison, DO concentrations in the upper 10 m of the water column during upwelling averaged 7.3 mg/L, 10% lower than during non-upwelling periods, which averaged 7.9 mg/L. The May 2019 DO measurement of 6.5 mg/L in the upper 10 m of the water column was 22% lower than historical average and the lowest value for a spring quarter since 1982; this low value is inconsistent with the typical trend, where higher DO levels in surface waters occur during upwelling events when compared to non-upwelling.

*pH*

Changes in the pH of receiving water due to the discharge of effluent are a concern because changes in pH can affect biological systems in many ways, such as reducing the ability of some organisms to produce calcareous shells. During 2018-2019, daily samples of JWPCP final effluent pH ranged from 6.9 to 7.1, with an average of 7.0 (LACSD 2019b, 2020c). At the edge of the ZID, pH reduction due to the effluent should be less than 0.05 pH units. By comparison, average receiving water pH between 31 and 60 meters ranged from 7.8 to 8.1 pH units (Table 2.1). Figure 2.4 shows the distribution pattern of pH in each quarter of 2018-2019. The pH data show that variability is primarily associated with vertical stratification, with declining pH at increasing depth in coastal waters off Palos Verdes. Some variability in surface pH distributions occurs between surveys, but no regular spatial patterns are apparent.

*Light transmission*

Change in the LT (turbidity) of receiving water due to the discharge of effluent is a concern because macro-algal growth could be impacted by reduced light energy penetration. During 2018-2019, daily samples of JWPCP final effluent

turbidity ranged from 2.7 to 7.4 NTUs (nephelometric turbidity units), with an average of 3.7 NTUs (LACSD 2019b, 2020c). For a 25 cm path-length transmissometer, readings from 20% to 80% are roughly equivalent to readings from 60 to 10 NTUs (Hydrolab 1997). Using the rough association that each NTU increase leads to a ~1% decrease in LT, the reduction in light transmission at the edge of the ZID due to the effluent should be less than 0.1%. By comparison average receiving water LT between 31 and 60 meters ranged by nearly 4% (86.1% to 90.3%; Table 2.1) between surveys in 2018-2019. Distribution patterns of LT for each quarter of 2018 and 2019 are shown in Figure 2.5. LT is not directly associated with upper ocean density stratification (Appendix 2.8). However, because phytoplankton concentrate in the euphotic zone, and sources of turbidity enter the ocean near the surface (coastal runoff, sediment resuspension by waves, etc.), increased LT is often correlated with increasing depth. In the surface layers, LT is also correlated with distance offshore, with clarity increasing away from shoreline sources of turbidity.

During 2018-2019, average LT in the upper 10 m of the water column ranged from 78.7% to 84.2%. A small number of very low (<60%) near surface LT measurements were made in most quarters. These lowest readings are due to highly turbid conditions at inshore sites due to stormwater runoff, or to resuspension of material above the bottom. In all quarters, surface LT is reduced near the coast, relative to offshore. Sites at harbor entrances and the San Gabriel River outlet show a pattern of reduced LT. Deeper offshore waters (61-100 m) were consistently clear, with average results for all quarters in 2018-2019 ranging from 87.9% to 91.4% (Table 2.1). Offshore, reduced LT correlates closely with sub-surface layers of CHL (Figures 2.5 and 2.6).

*Chlorophyll-a fluorescence*

The discharge of an effluent which contains nutrients into receiving water is a concern because of the potential for nuisance or harmful algal growth. Sanitation Districts' offshore surveys use an *in situ* CHLa fluorescence (CHL) sensor to assess algal concentrations and distribution patterns in the water column. When offshore surface features of elevated CHL are present, they generally map closely to areas of

reduced light transmission, confirming phytoplankton reduce the clarity of surface waters. Increased CHL may also correlate with areas where the DO and pH are elevated during the day, as a result of photosynthesis consuming carbon dioxide and producing oxygen.

Figure 2.6 shows 3D views of the distribution of CHL. In several quarters elevated surface CHL was observed at the inshore edge of the survey area, off the San Gabriel River mouth, and the LA-Long Beach harbor, and off the Palos Verdes coastline. Patchy surface distributions of CHL, extending offshore from these coastal features, were also observed.

Subsurface layers of elevated CHL were present in most quarters and represent the standing crop of phytoplankton located at the ideal depth for light, temperature and nutrient availability. At most sites, the maximum levels seen in the subsurface layer were significantly higher than surface levels. Overlaid vertical profiles of CHL in Appendix 2.6 show that the sub-surface layer varied considerably between sites on each survey, both the depth to peak concentrations, which ranged between the surface and 40 m, and the pattern of vertical distribution, with thin layers in some cases, and more vertically extended layers in others. Using the depth-bracketed mean values in Table 2.1, more than 80% of detected CHL within the survey area was located deeper than 10 m in 2018-2019.

*Ammonia*

Ammonia was measured on discrete samples, which were collected at selected depths from a subset of the offshore sites. In total, 89 permit required ammonia samples were collected each quarter. Because final effluent ammonia levels averaged 44.5 mg/L in 2018-2019, and the Sanitation Districts uses a low level ammonia method with an RL of 0.02 mg/L, levels of ammonia in seawater can be an effective indicator of the effluent plume at dilutions up to 2000:1. In 2018-19, 205 (29%) of samples contained ammonia at levels from 0.02 to 0.43 mg/L, another 42% of samples had ammonia below the Reporting Limit, but above the Method Detection Limit of 0.003 mg/L; 29% of samples were below the MDL. Ammonia was detected most frequently at the 15 m (39%) and 30 m (33%) depths. At the surface, ammonia was detected in only 12% of samples, at levels ranging from 0.02 to 0.12 mg/L.

During 2018-2019, the Sanitation Districts conducted a limited amount of non-permit required additional surface sampling for ammonia at three sites at the outer boundary of kelp growth on the Palos Verdes Peninsula (sites 2801, 2901, and 3101), and at a site directly in front of the mouth of the San Gabriel River (site 2501). Ammonia above the RL was not detected in any samples in front of the River but was detected in four of 24 kelp site samples. Even when detected, ammonia at these sites was only between 0.02 and 0.05 mg/L, while 84% of these inshore samples had no detected ammonia, which suggests that neither the River, nor the nearshore, are significant sources of ammonia.

*CDOM*

In 2018-2019, CDOM results clearly identified the subsurface effluent plume in every quarterly survey **(Appendix 2.9).** The CDOM patterns show that the effluent plume can move either upcoast or downcoast from the outfalls and may also move onshore or offshore. In many surveys, an effluent CDOM feature was present both upcoast and downcoast from the outfalls. These results are possible because along-shelf currents over the Palos Verdes shelf frequently reverse direction at tidal and diurnal time scales. In all surveys, the highest CDOM levels, and best-defined plume feature was associated with stations directly over, or adjacent to the JWPCP outfalls. CDOM in the coastal ocean can have sources other than the effluent. It is sometimes detected at nearshore sites, where runoff is present, and generally shows a gradual increase in background levels associated with increasing depth. CDOM may also be increased in areas with high CHL. Because of its strong signal, and association with the depth layers where the effluent is trapped, effluent CDOM can be statistically separated from these other sources.

**Compliance assessment**

By 1960, the Sanitation Districts had already accumulated 20 years of experience with installation and operation of multiport diffusers and had concluded that their use led to reductions in odor, discoloration, turbidity and bacterial levels in receiving waters (Rawn et al. 1959). The diffusers on the active 90- and 120-inch outfalls consist of several hundred small ports spaced at

intervals along the last approximately 1,000 m of the outfalls, in depths ranging from 50-70 m. Modeling studies predict that the buoyant plumes from each port should merge and stabilize within density-stratified layers of overlying water (Fischer et al. 1979). Models incorporating empirical data about the diffuser design, effluent properties, and ambient ocean conditions can accurately estimate initial dilutions of effluent (Muellenhoff et al. 1985). Roberts et al. (1989a, 1989b, 1989c) confirmed these theoretical results using scale models and field studies of multi-port diffusers with varying conditions of currents and stratification.

The JWPCP is permitted with a conservative static case dilution of 166:1, however actual dilution when factoring currents, variable stratification, and reduced effluent flows resulting from conservation efforts, is usually higher. Quantification of impact and assessment of compliance requires identifying areas where the dilute plume is present, as well as appropriate reference background waters for comparison.

*Plume detection*

Historical studies (Eppley et al. 1979; Thomas and Carsola 1980; Thomas et al. 1980), determined that ammonia is an effective tracer for dilute effluent plumes near ocean outfalls. Washburn et al. (1992) concluded, based on field studies on the Palos Verdes shelf, that to adequately map the effluent plume, distributions of multiple parameters need to be examined. More recently the Sanitation Districts and other SCB POTWs added CDOM fluorescence sensors to CTDs and have determined that *in situ* observation of CDOM is also an effective plume tracer, with the added benefit that results are instantaneous and continuous. **Appendix 2.10** includes inshore, outfall-crossing, and offshore transects for each 2018-2019 survey, for ammonia, CDOM, DO, and pH. Close agreement between ammonia and CDOM distribution patterns confirms their comparable ability to identify the plume. CDOM data are at the core of the effluent plume and reference site identification in the compliance tool.

The compliance tool was utilized to independently assess compliance with DO, pH and light transmission for each of the eight surveys completed in 2018 and 2019. **Figure 2.7** shows the subset of the 48-station offshore

sampling grid within the specified area defined by the compliance tool identified as Plume (red) and Reference (blue) using CDOM for each survey. Appendix 2.9 includes complete details of the settings, assumptions and results from use of the compliance tool for all eight surveys in 2018-2019.

**Appendix 2.11** includes quarterly outfall-crossing transects of CDOM, DO, and pH for surveys in 2018 and 2019, respectively. A subsurface peak of elevated CDOM can be seen proximal to the outfalls in each quarter. In all quarters, this core feature extends across-shelf both inshore and offshore (Appendix 2.10) of the outfall. In some quarters, areas of elevated mid-water CDOM and ammonia extend to survey boundaries, representing distances of 12 km upcoast and 21 km downcoast. In several quarters, separated areas of CDOM were apparent, which may indicate spatial and temporal limits of discrete sampling, separated plumes from the 90-inch and 120-inch outfalls, or separations of the effluent plume due to the diurnal flow cycle of effluent from JWPCP caused by tidal oscillations in local currents and vertical movements of density isotherms. It is also likely that on occasion the Sanitation Districts' sampling detects CDOM and ammonia from the major POTWs located upcoast and downcoast of the Palos Verdes peninsula. The variability in the patterns of CDOM and ammonia and the detection of elevated CDOM and ammonia many kilometers from the outfalls indicate the dynamic nature of processes driving far field advection of the dilute effluent plume.

*Effluent effects on ambient pH and DO*

The JWPCP NPDES permit contains numeric limits for the effects of discharged effluent on the ambient ocean pH and DO: pH shall not be changed at any time more than 0.2 units from that which occurs naturally as a result of discharge of waste, and the DO concentration shall not at any time be depressed more than 10% below that which occurs naturally as the result of the discharge of oxygen demanding waste (Order No., R4-2017-0180, Waste Discharge Requirements page 18; Appendix 1.2).

High spatial resolution sampling of DO and pH in the coastal ocean reveals distributions of these variables can be quite complex (Figures 2.3 and 2.4). Vertical density-controlled stratification, seasonal changes, upwelling

currents and phytoplankton blooms all contribute to the distributions of these variables in the ocean off Palos Verdes. Determining the natural level of these variables at any particular location, depth,

and time of year is not straightforward. Since neither the NPDES permit nor the COP provide explicit procedures for determining compliance, SCCWRP, in collaboration with the Sanitation Districts and other SCB POTWs, developed the analytical procedures described previously to assess compliance with these standards in the SCB.

The relatively warmer and freshwater effluent is significantly less dense than the ocean receiving water at a depth of 60 m. As a result, it rises rapidly, while simultaneously mixing with ambient receiving water. Entrainment and upward movement of water by the typical 20-40 m rise of the effluent into the water column further complicates the quantification of the direct DO reduction due to the effluent. This hydraulic effect, predicted by models, has been observed by researchers (Wu et.al.1994; Washburn et. al. 1992) and is likely to be a more significant contributor to localized reductions in DO concentration in the mid-water than the BOD of the effluent. The compliance assessment tool includes an algorithm to account for the effect of entrainment.

**Table 2.3** summarizes the depth and greatest maximum oxygen reduction at each of the identified Plume sites in each quarter of 2018 and 2019. The calculated reduction in oxygen exceeded the 10% criteria twice: one in the summer quarter of 2018 and once in fall quarter of 2019. These were both investigated and appear to be due to natural stratification of the water column from high sea surface temperature reducing the mixing of oxygenated surface waters and deeper waters. The same trends are evident at each site during strong stratification events in previous years when the plume was absent from the site, indicating that these results were likely not caused by the effluent plume. Therefore, these exceedances do not represent violations of the permit limit. Decreases in oxygen relative to the reference were identified at 23 of 32 plume sites and ranged from 0.44 to 16.2%. At the remaining 9 plume sites increases in oxygen relative to the reference were determined, with a maximum increase of 4.87%. The average change in oxygen for all 32 sites was -3.62%.

Maximum reductions in pH at all 39 Plume sites were separately determined by the compliance program algorithm (Table 2.3). None of the decreases exceeded the 0.2 pH unit criteria. Deceases relative to the Reference value were observed at 16 of 32 sites and ranged from 0.002 to 0.018. At the remaining Plume sites, the pH was unchanged or increased relative to the Reference, with a maximum increase of 0.009. The average change in pH for all 32 sites was -0.003 pH units.

*Effluent effects on offshore LT*

The compliance tool includes a function to test whether a statistically significant difference (95th percentile) exists between two groups of data. This feature was used to compare mean LT values measured at the combined Plume sites with the Reference sites. Table 2.3 shows that the mean LT levels were statistically lower in the Plume in all eight surveys. The average reduction for all eight quarters was 2.4%, which is less than the natural variability observed within the reference sites during the monitoring period. Further, mean Plume levels of LT were relatively high, at 85.7%, while Reference levels were 87.8%. Typically, the clearest offshore waters seen off Palos Verdes have LT values at approximately 90%, which was the maximum of the Reference. The maps in Figure 2.7 show that many Reference sites were further from shore than Plume sites, and since LT is roughly inversely correlated with distance from shore this could be a partial explanation. When the JWPCP moved to full secondary treatment, levels of dissolved solids and turbidity were reduced significantly. Present levels are over an order of magnitude lower than during the era of Primary treatment. Nonetheless, field experiments have shown that in a representative sample of coastal ocean seawater, adding as little as one part of secondary effluent in 2000 parts of seawater produced a very small but statistically significant reduction in LT.

In addition to monitoring LT at the offshore sites, the Sanitation Districts measure PAR energy at seven nearshore sites monthly. The purpose of this monitoring is to assure that transmission of natural light is within ranges needed to ensure the protection of benthic algal communities. The nearshore light energy data are discussed in more detail in the section 'effluent effects on natural light levels' below.

# Table 2.3 Water Column Assessment: Oxygen, pH, and light

Change in dissolved oxygen and pH at each plume site are shown relative to the Reference site. Mean values of light transmittance at Reference and all plume sites are compared, and statistical significance of the difference is listed. Red sites are calculated DO outranges.* The Plume was significantly higher than Reference.

| Year | QTR | Reference Sites | Plume Sites | Change in Dissolved Oxygen (%) | Depth (m) | Change in pH (value) | Depth (m) | Mean %T Reference | Mean %T Plume | Statistically Significant (95%) |
|------|-----|-----------------|-------------|-------------------------------|-----------|---------------------|-----------|-------------------|---------------|--------------------------------|
| 2018 | Q1 | 2702-1, 2802-1, 2803-1, 2804-1, 2805-1, 2806-1, 2904-1, 2905-1, 2906-1, 3005-1, 3006-1 | 3003-1 | -5.90 | 29.5 | -0.011 | 32.0 | 87.74 | 85.77 | Yes |
|      |    |                 | 3053-1 | -5.34 | 24.0 | -0.010 | 26.9 | | | |
|      |    |                 | 3105-1 | -4.32 | 23.0 | -0.003 | 45.7 | | | |
| 2018 | Q2 | 2702-1, 2805-1, 2806-1, 2904-1, 2905-1, 2906-1, 3004-1, 3005-1, 3006-1, 3054-1 | 2705-1 | -4.45 | 36.8 | 0.001 | 40.7 | 88.24 | 86.56 | Yes |
|      |    |                 | 2802-1 | -6.03 | 22.5 | -0.005 | 24.3 | | | |
|      |    |                 | 2803-1 | -1.65 | 34.8 | 0.000 | 38.8 | | | |
|      |    |                 | 2804-1 | 2.70 | 31.9 | 0.002 | 97.9 | | | |
|      |    |                 | 2902-1 | -0.44 | 24.8 | -0.005 | 24.8 | | | |
|      |    |                 | 3002-1 | -6.26 | 25.8 | -0.008 | 24.7 | | | |
|      |    |                 | 3003-1 | -2.92 | 15.2 | -0.005 | 22.0 | | | |
|      |    |                 | 3103-1 | -0.83 | 35.8 | -0.006 | 37.2 | | | |
| 2018 | Q3 | 2702-1, 2803-1, 2804-1, 2805-1, 2806-1, 2904-1, 2905-1, 2906-1, 3005-1, 3006-1 | 2902-1 | -16.19 | 25.3 | -0.015 | 22.9 | 88.14 | 86.21 | Yes |
|      |    |                 | 2904-1 | -8.12 | 24.7 | -0.008 | 17.7 | | | |
|      |    |                 | 2905-1 | -8.49 | 25.7 | -0.008 | 27.7 | | | |
|      |    |                 | 2906-1 | -5.65 | 26.5 | -0.004 | 28.8 | | | |
|      |    |                 | 3003-1 | -8.01 | 59.0 | -0.018 | 29.7 | | | |
|      |    |                 | 3053-1 | -8.05 | 45.8 | -0.008 | 45.2 | | | |
| 2018 | Q4 | 2803-1, 2804-1, 2805-1, 2904-1, 2905-1, 2906-1, 3003-1, 3005-1, 3006-1 | 2903-1 | 1.61 | 45.8 | 0.000 | 56.2 | 87.35 | 84.82 | Yes |
| 2019 | Q1 | 2804-1, 2805-1, 2904-1, 2905-1, 2906-1, 3004-1, 3005-1, 3006-1 | 2803-1 | 2.93 | 45.2 | 0.000 | 45.2 | 87.40 | 85.62 | Yes |
| 2019 | Q2 | 2804-1, 2805-1, 2904-1, 2905-1, 2906-1, 3002-1, 3004-1, 3005-1 | 2702-1 | -3.43 | 23.0 | 0.000 | 23.0 | 90.11 | 87.11 | Yes |
|      |    |                 | 2802-1 | -6.77 | 27.8 | -0.002 | 26.8 | | | |
|      |    |                 | 2803-1 | -1.97 | 22.9 | 0.000 | 58.8 | | | |
|      |    |                 | 3003-1 | 0.48 | 23.8 | 0.001 | 23.8 | | | |
|      |    |                 | 3006-1 | 0.63 | 87.8 | 0.000 | 92.8 | | | |
| 2019 | Q3 | 2803-1, 2804-1, 2805-1, 2904-1, 2905-1, 2906-1, 3004-1, 3005-1, 3006-1 | 2902-1 | 1.39 | 27.8 | -0.002 | 23.8 | 87.11 | 84.69 | Yes |
|      |    |                 | 3002-1 | 4.87 | 14.2 | 0.001 | 27.3 | | | |
|      |    |                 | 3003-1 | 0.93 | 47.5 | 0.001 | 26.2 | | | |
|      |    |                 | 3053-1 | 1.23 | 57.0 | 0.000 | 42.3 | | | |
| 2019 | Q4 | 2905-1, 2906-1, 3004-1, 3005-1, 3006-1 | 3003-1 | -4.42 | 29.7 | 0.000 | 41.9 | 86.73 | 85.01 | Yes |
|      |    |                 | 3052-1 | -10.90 | 17.0 | 0.002 | 29.8 | | | |
|      |    |                 | 3053-1 | -6.93 | 17.0 | 0.002 | 42.0 | | | |
|      |    |                 | 3103-1 | -5.63 | 39.2 | 0.009 | 59.2 | | | |

*Effluent effects on chlorophyll*

The permit requires that the effluent not contain nutrients at levels that will cause objectionable aquatic growths or degrade indigenous biota. The JWPCP effluent does contain considerable levels of nutrients, particularly nitrogen in the form of ammonia. As described earlier, the Sanitation Districts use an *in situ* CHLa fluorometer to assess the concentration

and distribution patterns of phytoplankton in the offshore waters. In 2018 and 2019, no consistent along-shelf or cross-shelf trends, indicative of discharge related impacts, were apparent in the CHL distributions. The highest average CHL levels in 2018-2019 were observed in the February 2018 survey, but highest maximum levels were observed in the August 2019 survey. CHL levels throughout each quarter were similar throughout all 2018-2019, with some seasonal variation in surface waters. No observations of objectionable aquatic growths were seen during any offshore surveys during 2018 and 2019.

Assessing the ultimate effect of POTW nutrients both on primary productivity, as well as on ocean acidification and hypoxia (OAH) is a non-trivial effort. In 2016 a west-coast wide consortium began development of a linked physical-biogeochemical model to investigate the possible effects.

*Effluent effects on natural light levels*

Measurements of PAR were made monthly from the surface to 18 m at seven nearshore sites (L1-L7). PAR measurements give a quantitative indication of the amount of light reaching different depths in the nearshore regions. This direct measurement of natural light transmission was evaluated against the NPDES permit requirement that natural light not be reduced to levels that suppress benthic macroalgal growth (Order No. R4-2017-0180, page E-28). The dominant rocky subtidal community along the Southern California coast is the kelp forest, and adequate light level is a critical environmental indicator of conditions that allow kelp to become established and thrive.

**Figure 2.8** compares the historical average percent of light energy reaching the 18 m bottom depth at each nearshore site for 1982-2019 with
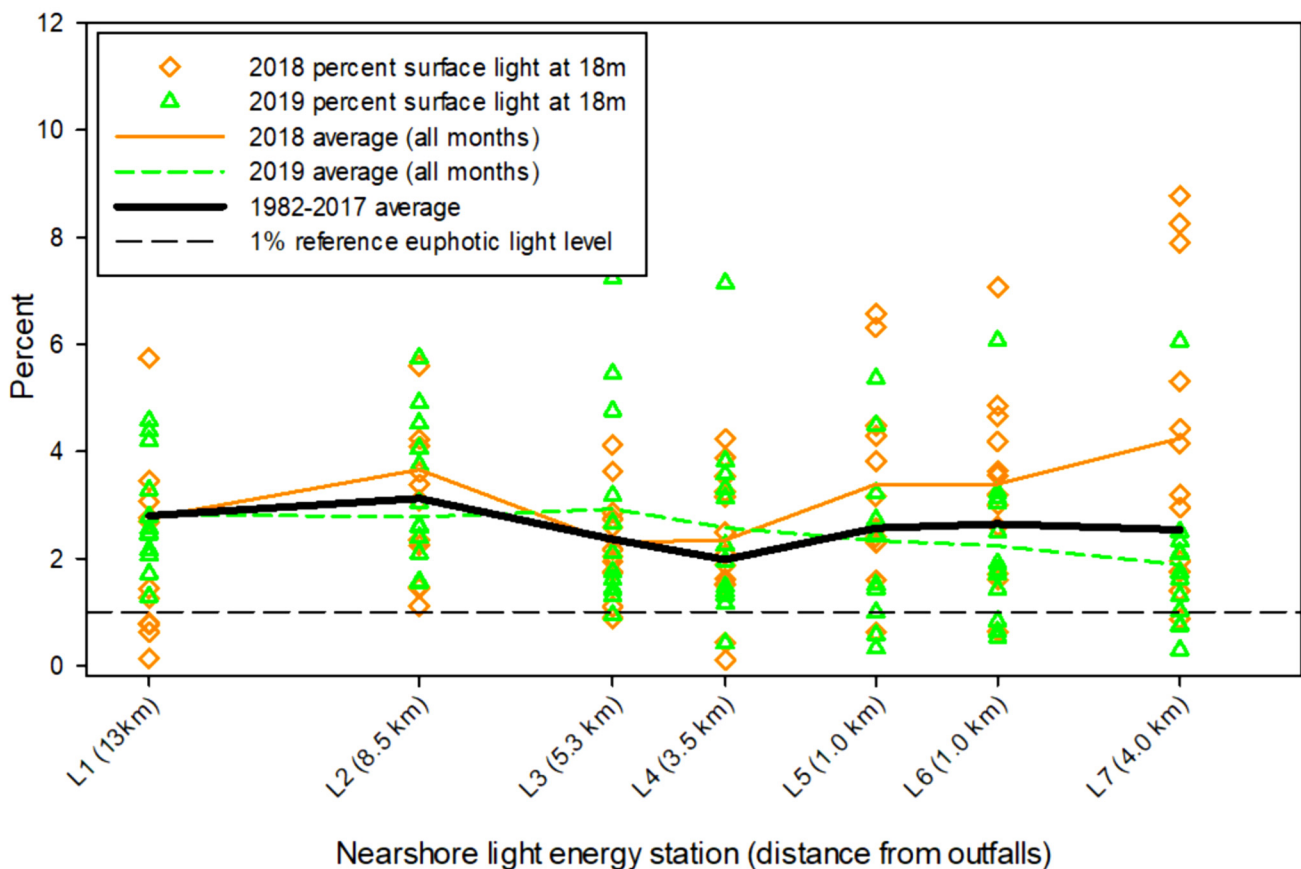


## Figure 2.8 Percent of Light Energy Reaching the Bottom

The measured percent of surface light energy reaching 18m at nearshore stations each month of 2018 and 2019 are plotted. The average percentage of surface light energy reaching 18m bottom depths is plotted with an orange line (2018) and a dashed green line (2019). The historical average levels for 1982-2015 are plotted as a heavy black line. The distance from the outfalls to each nearshore site is shown on the axis label. The 1% reference (euphotic) level is plotted as a dashed black line.

the average levels in 2018 and 2019. Also shown on Figure 2.8 are the 18 m light levels for each monthly survey in 2018 and 2019. At most nearshore sites there are a few months, mostly during the winter for 2018, where the 18 m light level was measured at less than the 1% euphotic light level. These are months when storm surf and stormwater runoff are expected to have the greatest effect on water clarity in the nearshore. There are also months in the middle of the year that have less than the 1% euphotic light level due to red tide being present at the time of sampling. The points in Figure 2.8 correspond with the tabular summary in Table 2.2, where the month/sites with less than 1% light energy at 18 m are highlighted. If more than 1% of light is available, then the water is considered to be within the euphotic zone, where the rate of photosynthesis exceeds the rate of respiration (Eppley et al. 1979). In 2018-2019 the average percent of light energy reaching 18 m was 2.8%, more than twice the euphotic target. Table 2.2 also confirms that in 2018 and 2019, all light energy sites had average levels greater than 1% except in December of 2018. These levels are considered sufficient to support normal growth of benthic macroalgae.

Direct assessment of the Palos Verdes kelp beds by the Central Region Kelp Survey Consortium (CRKSC) confirms these findings. The CRKSC completes quarterly surveys of kelp bed coverage along the Southern California coastline. These quantitative surveys allow recent kelp bed extent to be compared with historical levels. For the peak quarters in 2018 and 2019, kelp coverage on the Palos Verdes Peninsula was 4.78 km$^2$ and 1.72 km$^2$, respectively. The coverage number for 2018 is significantly above levels in most years since the 1980s and was the highest since CRKSC surveys began in 2003. The kelp coverage for 2019 declined across the entire region as sea surface temperatures remained high and nutrient availability was the lowest recorded since 2015. Relative to historical levels in the SCB, kelp coverage around the Palos Verdes Peninsula is comparable to areas away from the outfalls (MBC Applied Environmental Sciences 2020).

Although overall light levels were sufficient to support growth, clear spatial patterns of light energy exist along the Palos Verdes coastline. The net subsurface current over the central Palos Verdes shelf, above the diffusers, is typically upcoast. However, the nearshore surface current off the Palos Verdes headland often moves downcoast. Erosion of coastal material, particularly from the area of the Portuguese Bend landslide, located between nearshore sites L3 and L4 in Figure 2.2, can lead to significant nearshore turbidity which is most commonly carried eastward. Since it began in 1956, the landslide has contributed between 5.7–9.4 million metric tons of sediment to the Palos Verdes shelf, more than twice the loading from the effluent discharge (Kayen et al. 2002). This input may explain the slight reduction in light energy at site L4, located east of the landslide area.

**Temporal trends**

*Offshore water column trends, 1988-2019*

An analysis of the water quality data from thirty years of CTD surveys was completed for this report. Data from the 30 m depth of two sites was used in the analysis of temporal trends. Site 2903 is located within the ZID where the effluent plume is frequently present. Site 3103 is about 12 kilometers away from the discharge site on the same 60 m isobath as site 2903. Site 3103 is used as a reference site to contrast the effluent discharge effects at site 2903. **Figure 2.9** compares the DO and pH results from the ZID and reference sites in three different ways: 1) a time series of the measured results from each site (plots A and D), 2) the average quarterly cycle of monthly levels at each site (plots B and E), and 3) scatterplots of the ZID versus reference data in the context of the effluent plume as measured by ammonia (plots C and F).

The time series show a possible twenty-year cycle in DO and pH, with the most recent peak around 2015. DO and pH levels in 2018 and 2019 remain near long term average levels. For the period 1988-2019, the average value of DO at the ZID site, 6.8 mg/L, is just 0.2 mg/L or 3% lower than the reference site value of 7.0 mg/L. By comparison the DO values at the reference site range from 3.0 to 9.8 mg/L over this time period. This natural variability at the reference site is approximately 30 times greater than the average difference between the ZID and the reference site.

The average annual cycle of DO at the reference site ranges from a low of 5.7 mg/L in the spring quarter, reflecting the effect of spring upwelling, to higher and more consistent levels of 7.5, 7.5, and 7.4 mg/L in summer, fall, and winter
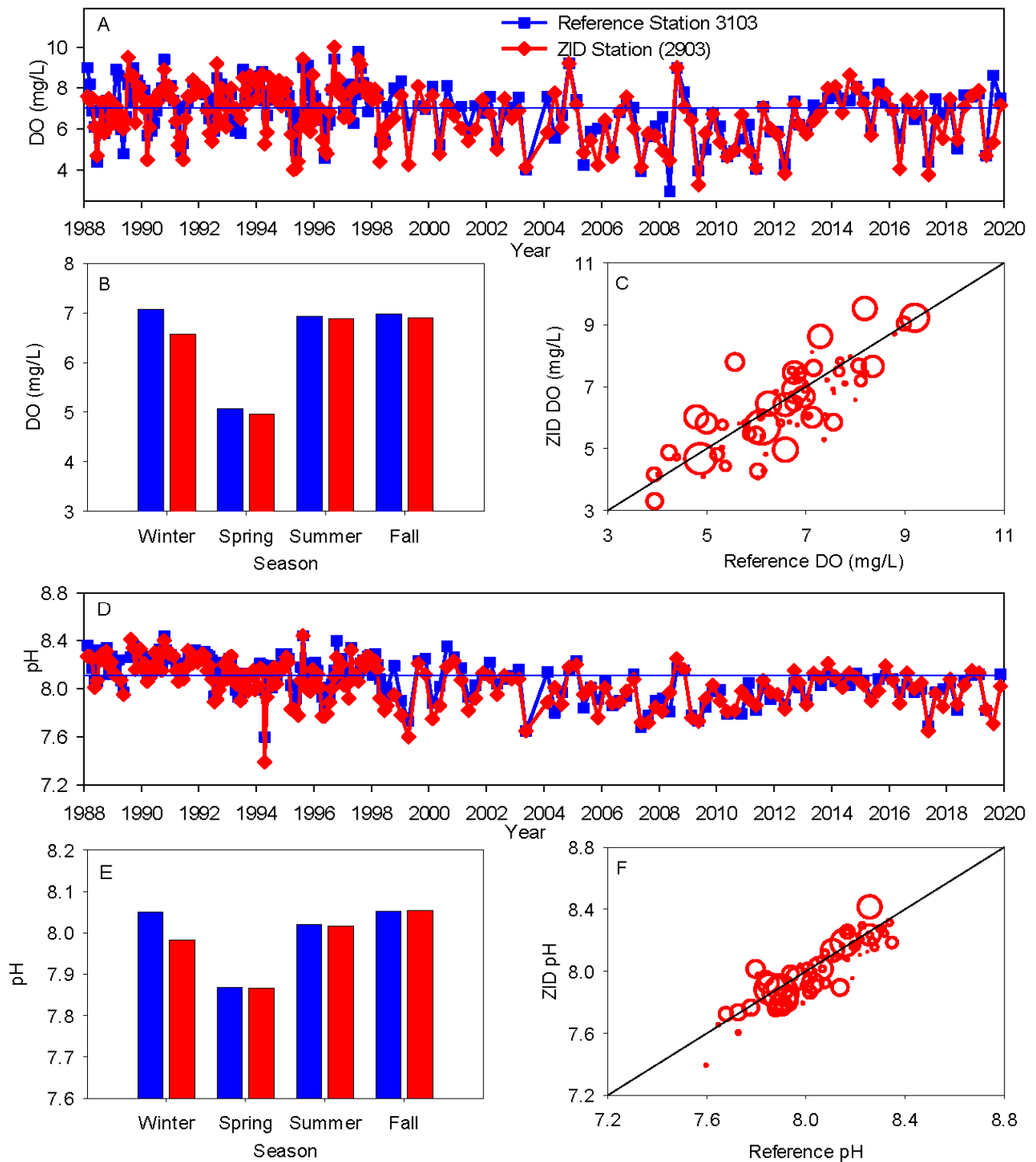
## Figure 2.9 Temporal Patterns in DO and pH

Palos Verdes water column time series of dissolved oxygen (DO) and pH at the 30m depth of reference site 3103 and ZID site 2903 (A and D), average annual cycle of DO and pH (B and E) at the reference and ZID sites, and scatterplot of reference versus ZID DO and pH (C and F) for 1988-2019. Straight blue line shows reference site mean for comparison (A,B, D, and E). When it was measured at 30m, the ZID station ammonia concentration is shown as the circle diameter on the scatterplots of DO and pH.

surveys, respectively. This average annual seasonal range in DO at the reference site is about eight times greater than the average difference between the ZID and the reference site. The scatterplot of ZID versus reference site DO illustrates that DO concentration between these sites is closely correlated. Further, the levels of ammonia that were measured simultaneously with the DO at the ZID site show no pattern that would suggest DO levels are lower within the plume or correlated with plume concentration.

On average, the ZID pH was 0.04 pH units lower than the reference (Figure 2.9, D and F). By comparison the range of pH values observed at the reference site from 1988 to 2019 is 7.60 to 8.44 pH units. The natural range of pH at the reference site is approximately 20 times greater than the average difference between the ZID and the reference site. The average annual cycle of pH at the reference site ranges from a low of 7.98 in the spring quarter, reflecting the average effect of spring upwelling, to higher and more consistent levels of 8.11, 8.16, and 8.15 in summer, fall and winter quarters, respectively. This average annual seasonal range in pH at the reference site is about four times greater than the average difference between the ZID and reference. The scatterplot of ZID versus reference site pH shows a tight linear grouping and confirms the consistent close agreement of results from individual sampling events between these two sites. The levels of ammonia that were measured simultaneously with the pH at the ZID site show no pattern that would suggest pH levels are lower within the plume or correlated with plume concentration. **Appendix 2.11** includes directly comparable time series plots of temperature, salinity, and light transmissivity for the period 1988–2019 at the 30 m depth at sites 2903 and 3103. Differences in temperature and salinity between the ZID and reference sampling points are much less than the seasonal and inter-year variability revealed in these time series. The temperature time series shows that after a strong El Nino effect of warmer water in 1998, observed temperatures varied in a range between zero and two degrees below long term averages until beginning a gradual increase in 2011, which peaked in 2015 and has declined slightly (approximately one degree) through 2019. An apparent decadal cycle in salinity, between 1988 and 2008, has over the last decade, flattened out, with smaller cyclical oscillations of 1-2 year duration since 2012. The decadal cycle varied by

about 0.4 ppt. LT has stayed relatively constant between 1988 and 2019. LT at the ZID site has on average been about 2% lower than the reference. Levels at the ZID appear to have increased by about 1% around the time the JWPCP began full secondary treatment, which led to a decrease in effluent suspended solids from 70 mg/L to 15 mg/L, and a corresponding decrease in final effluent turbidity from around 50 NTUs to 6 NTUs.

*Nearshore light energy trends, 1982-2019*

Seven nearshore light energy sites at fixed locations along the 18 m isobath have been surveyed monthly since 1982. Using this data set, trends in light energy penetrating to the bottom, water clarity, and water color are examined. The principal observation made at these sites is the amount of PAR reaching to the bottom at 18 m.

**Figure 2.10** shows that the annual average percent of surface light reaching to 18 m has ranged from 1.6% to 4.6%. In all years the annual average PAR reaching the bottom has been above the 1% euphotic level needed to allow primary production and growth of macroalgae. Superimposed on the overall average line in Figure 2.10 are the annual average values at sites L5 and L6, which are nearest to the outfalls, and site L4 which is directly down current from the Portuguese Bend landslide. In 2018 and 2019, the average annual light energy levels remained at typical long-term average levels.

### CONCLUSIONS

All Nearshore and Offshore Water Quality Monitoring required by the NPDES permit was completed in 2018 and 2019. The data from these surveys were submitted in 2019 and 2020 in annual receiving water data summary reports. The appendices included with this report provide field observational sheets, and additional graphical representations for the 2018 and 2019 CTD, ammonia, and light energy data. Results from the quarterly CTD surveys completed in 2018 and 2019 indicate that parameters were within normal annual ranges, and that seasonality was consistent with earlier years.

Spatial assessment of the CTD data found that the values of temperature, salinity, DO, and pH are most strongly associated with depth, although these parameters also vary seasonally. A

sub-surface salinity feature that forms below the thermocline during summer and fall months was noted as an exception. Extremes of low temperature and high salinity at depth occur during upwelling events in spring. During upwelling events, annual minimum values of DO at sub-thermocline depths were also observed. A layer of phytoplankton at the base of the pycnocline was observed nearly year-round, at depths ranging from less than 10 m to 40 m. Based on depth weighted averages, 80% of the CHLa fluorescence seen in 2018-2019 was located deeper than 10 m.

A localized feature of reduced light transmittance and salinity and elevated chlorophyll is routinely observed in surface waters off the mouth of the San Gabriel River, and sometimes extending in front of the Los Angeles/Long Beach Harbor complex. For 2018 and 2019, the Sanitation Districts used the SCCWRP compliance tool for DO, pH, and LT. Using CDOM data, the tool identified the plume

over the outfalls in every quarter. In the summer quarter of 2018 and fall quarter of 2019 DO was found to be out of range at one site each, 2902 and 3052 respectively. These appear to be due to natural stratification of the water column from high sea surface temperature reducing the mixing of oxygenated surface waters with deeper waters; similarly low values have also been observed at these sites during strong stratification events in previous years, even when the plume was absent, indicating that these results were likely not caused by the effluent plume and are not violations of the permit limit. No other out of range occurrences of either DO or pH were determined in 2018-2019. Offshore LT levels were significantly (2-tailed t-test at 95%) lower in the plume than the reference in all eight quarters. Although significant, the overall average difference was only about 2%, and the available PAR light energy at nearshore sites was within ranges to support benthic macroalgae. Offshore water column CHL distributions showed no increase associated with
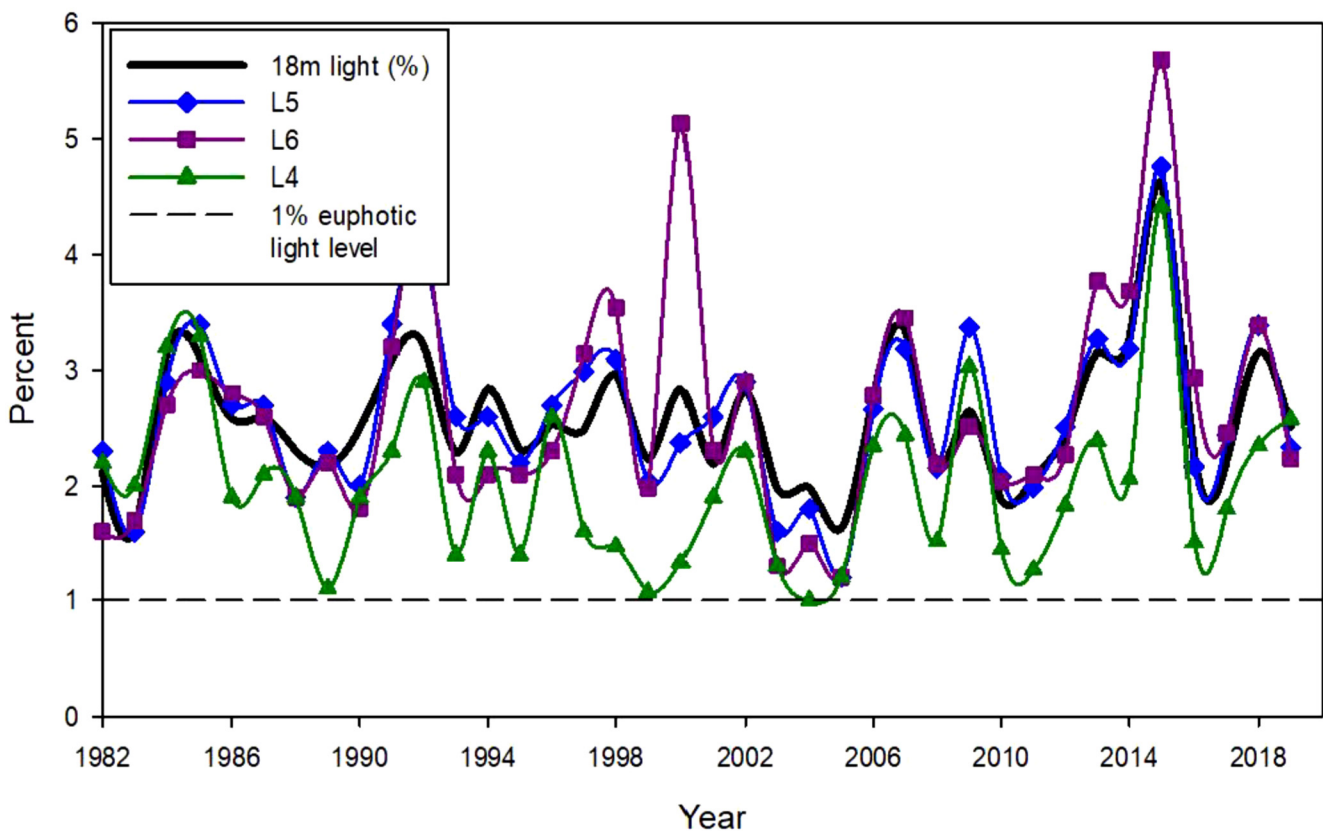


## Figure 2.10 Temporal Patterns in Light Energy

Comparison of the annual average percent of PAR reaching 18m for all nearshore stations in each year for 1982 – 2019. Data for three individual sites are also plotted; L5 and L6 are the nearest stations to the outfalls, and station L4 is adjacent to the Portuguese Bend landslide which has increased nearshore turbidity. The one percent reference (euphotic) level is plotted as a dashed black line.

the effluent plume, and no observations of objectionable aquatic growths or degradation of indigenous biota were made during 2018-2019. There was no quantitative or qualitative observation of eutrophication.

A comparison of 30 years of CTD data focused on DO and pH at 30 m depth at a ZID and reference site determined the ZID site is only minimally affected by the discharge. Natural DO and pH variability are much greater than the small differences between the ZID and reference sites.

The annual average levels of light energy reaching the bottom at nearshore sampling sites have stayed above the 1% euphotic light level for the last 37 years. Sites nearest the outfalls are not significantly different from the overall average. In 2018-2019 light levels remained close to longer term average levels.

## LITERATURE CITED

Baumgartner DJ, Frick WE, Roberts PJW. 1994. Dilution models for effluent discharges. 3rd ed. Washington, D.C. Office of Research and Development, U.S. Environmental Protection Agency. Report No.: EPA/600/R-94/086

Dorman CE, Palmer DP. 1981. Southern California summer coastal upwelling. In: F.A. Francis, editor. Coastal Upwelling. Coastal and Estuarine Sciences. AGU, Washington, D.C. 1:44-56

Eppley RW, Renger EH, Harrison WG, Cullen JJ. 1979. Ammonium distribution in Southern California coastal waters and its role in the growth of phytoplankton. Limnology and Oceanography. 24(3):495-509.

Fischer HB, List EJ, Koh RCY, Imberger J, Brooks NH. 1979. Mixing in inland and coastal waters. San Diego (CA), Academic Press. 483 p.

Hendricks TL. 1974. Measurements of coastal currents. In: W. Bascom (Proj. Dir.), Southern California Coastal Water Research Project Annual Report, 1974. El Segundo, Calif. pp. 153- 158.

Hendricks TL. 1975. Properties of nearshore currents. In: W. Bascom (Proj. Dir.), Southern California Coastal Water Research Project Annual Report, 1975. El Segundo, Calif. pp. 167-172.

Hendricks TL 1982. Shelf and slope currents off Newport Beach. In: W. Bascom (ed.), Southern California Coastal Water Research Project Biennial Report, 1981-1982. Long Beach, Calif. pp. 237-245.

Hydrolab Inc. [Internet] 1997. Technical note#206: transmissivity. [cited April 19, 2012]. Available from: http://www.panwell- tech.com/panwell/techdoc/hydrolab/ Transmissivity.pdf

Jones B, Bratkovich A, Dickey T, Kleppel G, Steele A, Iturriaga R, Haydock I. 1986. Scales of variability in physical, chemical and biological parameters in the vicinity of an ocean outfall. Stratified Flows, Proceedings of the Third International Conference on Stratified Flows. 1987 Feb 3-5. Pasadena (CA). American Society of Civil Engineers.

Jones B, Noble MA, Dickey TD. 2002 Hydrographic and particle distributions over the Palos Verdes continental shelf: Spatial, seasonal and daily variability. Continental Shelf Research. 22:945-965

Kayen RE, Lee HJ, Hein JR. 2002. Influence of the Portuguese Bend landslide on the character of the effluent-affected sediment deposit, Palos Verdes margin, southern California. Continental Shelf Research. 22:911-922

[LACSD] Los Angeles County Sanitation Districts. 2008. Palos Verdes flow study 2000-2008 final report. Whittier, CA: Los Angeles County Sanitation Districts, Ocean Monitoring and Research Group, Technical Services Department.

[LACSD] Los Angeles County Sanitation Districts. 2019a. 2018 annual receiving water data summary report [compact disk]. Whittier, CA: Los Angeles County Sanitation Districts, Ocean Monitoring and Research Group, Technical Services Department.

[LACSD] Los Angeles County Sanitation Districts. 2019b. JWPCP annual NPDES monitoring report for 2018. Whittier, CA: Los Angeles County Sanitation Districts, Treatment Plant Monitoring Group, Technical Services Department.

[LACSD] Los Angeles County Sanitation Districts. 2020a. JWPCP biennial receiving water monitoring report 2018-2019. Whittier, CA: Los Angeles County

Sanitation Districts, Ocean Monitoring and Research Group, Technical Services Department.

[LACSD] Los Angeles County Sanitation Districts. 2020b. 2019 annual receiving water data summary report [electronic file]. Whittier, CA: Los Angeles County Sanitation Districts, Ocean Monitoring and Research Group, Technical Services Department.

[LACSD] Los Angeles County Sanitation Districts. 2020c. JWPCP annual NPDES monitoring report for 2019. Whittier, CA: Los Angeles County Sanitation Districts, Treatment Plant Monitoring Group, Technical Services Department.

MBC Applied Environmental Sciences. 2020. Status of the kelp beds 2019, Ventura and Los Angeles Counties. Whittier, CA: Central Region Kelp Survey Consortium.

Muellenhoff WP, Soldate AM, Baumgartner DJ, Schult MD, Davis LR, Frick WE. 1985. Initial mixing characteristics of municipal ocean discharges. Vol. 1, procedures and applications. Narragansett (RI). Environmental Research Laboratory, U.S. Environmental Protection Agency. Report No.: EPA-600/3-85-073a.

Nezlin NP, Booth JAT, Beegan C, Cash CL, Gully JR, Latker A, Mengel MJ, Robertson GL, Steele A, Weisberg SB. 2016. Assessment of wastewater impact on dissolved oxygen around southern California's submerged ocean outfalls. Regional Studies in Marine Science, In Press.

Rawn AM, Bowerman FR, Brooks NH. 1959. Diffusers for disposal of sewage in sea water. American Society of Civil Engineerrs, Sanitary Engineering Division 86(SA 2):65-105.

Roberts PJW, Snyder WH, Baumgartner DJ. 1989a. Ocean outfalls I: submerged wastefield formation. Journal of Hydraulic Engineering. 115(1):1-25.

Roberts PJW, Snyder WH, Baumgartner DJ. 1989b. Ocean outfalls II: spatial evolution of submerged wastefield. Journal of Hydraulic Engineering. 115 (1):26-48.

Roberts PJW, Snyder WH, Baumgartner DJ. 1989c. Ocean outfalls III: effect of diffuser design on submerged wastefield. Journal of Hydraulic Engineering. 115 (1):49-70.

Thomas WH, Carsola AJ. 1980. Ammonium input to the sea via large sewage outfalls. Part 1: tracing sewage in Southern California waters. Marine Environmental Research. Vol. 3:277-289.

Thomas WH, Hastings J, Fujita M. 1980. Ammonium input to the sea via large sewage outfalls. Part 2: effects of ammonium on growth and photosynthesis of Southern California phytoplankton cultures. Marine Environmental Research. 3:291-296.

Washburn L, Jones BH, Bratkovitch A, Dickey TD, Chen MS. 1992. Mixing, dispersion and resuspension in vicinity of ocean wastewater plume. Journal of Hydraulic Engineering. 113 (1):38-58.

Winant CD. 1983. Longshore coherence of currents on the Southern California shelf during the summer. Journal of Physical Oceanography. 13(1):54-64.

Winant CD, Bratkovich A. 1981. Temperature and currents on the Southern California shelf: a description of the variability. Journal of Physical Oceanography. 11:71-86.

Wu Y, Washburn L, Jones BH. 1994. Buoyant plume dispersion in a coastal environment: evolving plume structure and dynamics.

This page intentionally left blank